
Updated information and services can be found at:
<http://jb.asm.org/content/174/18/5895>

CONTENT ALERTS

These include:

Receive: RSS Feeds, eTOCs, free email alerts (when new articles
cite this article), [more»](#)

Information about commercial reprint orders: <http://jb.asm.org/site/misc/reprints.xhtml>
To subscribe to to another ASM Journal go to: <http://journals.asm.org/site/subscriptions/>

Origin, Structure, and Regulation of *argK*, Encoding the Phaseolotoxin-Resistant Ornithine Carbamoyltransferase in *Pseudomonas syringae* pv. phaseolicola, and Functional Expression of *argK* in Transgenic Tobacco

EFSTATHIOS HATZILOUKAS¹ AND NICKOLAS J. PANOPOULOS^{2*}

Department of Plant Pathology, University of California, Berkeley, California 94720,² and Institute of Molecular Biology and Biotechnology, Foundation for Research and Technology-Hellas, and Department of Biology, University of Crete, Heraklio, Greece¹

Received 12 November 1991/Accepted 9 July 1992

Pseudomonas syringae pv. phaseolicola produces the tripeptide $N^6(N'$ -sulfo-diaminophosphinyl)-ornithyl-alanyl-homoarginine (phaseolotoxin), which functions as a chlorosis-inducing toxin in the bean halo blight disease by inhibiting ornithine carbamoyltransferase (OCT). The bacterium possesses duplicate OCT genes, one of which, *argK*, encodes a toxin-resistant enzyme (ROCT) and imparts resistance to phaseolotoxin. We sequenced the *argK* gene from strain NPS3121, defined its promoter region, analyzed its regulation, and characterized its transcripts. The gene probably originated from another organism, since it is very distantly related to the *argF* gene encoding the housekeeping toxin-sensitive OCT and has low G+C content compared with the bacterial genome as a whole and with other protein-coding genes from *P. syringae* pv. phaseolicola. Optimized alignments of 13 OCT sequences allowed us to define key residues that may be responsible for toxin resistance and to identify a distinct prokaryotic amino acid signature in ROCT, which argues for a prokaryotic origin of *argK*. An in-frame fusion of the *argK* coding region with the chloroplast transit peptide segment of the pea *rbcs* gene was introduced in *Nicotiana tabacum* by *Agrobacterium*-mediated transformation. The presence of an ROCT activity in transgenic plants was demonstrated by in vitro and in vivo assays. Some plants were toxin resistant, suggesting that pathogen-derived resistance to the toxin should be feasible in the pathogen's host.

Bacterial pathogens of agronomic plants often produce low-molecular-weight toxins that function as virulence or pathogenicity determinants (15, 53, 61, 62). Toxigenic strains (Tox⁺) of *Pseudomonas syringae* pv. phaseolicola growing at temperatures of 18 to 22°C produce phaseolotoxin [$N^6(N'$ -sulfo-diaminophosphinyl)-ornithyl-alanyl-homoarginine (55)], which functions as a chlorosis- and growth retardation-inducing toxin in the bean halo blight disease (53). This toxin and its nonpeptide derivative [$N^6(N'$ -sulfo-diaminophosphinyl)-ornithine, trivial name octicide (55)] are potent inhibitors of ornithine carbamoyltransferases (OCTs) (15, 53). Octicide is a transition-state analog, causing irreversible inhibition of OCT, while phaseolotoxin inhibits the enzyme reversibly (53, 82). A total of 17 different OCTs that have been tested (7 bacterial, 9 from plants, and the rat liver enzyme) are all sensitive to octicide and/or to phaseolotoxin in vitro and/or in vivo (18).

Toxigenic strains of *P. syringae* pv. phaseolicola possess a unique form of OCT that is tolerant to phaseolotoxin and octicide, in addition to an OCT that is sensitive to these inhibitors (15, 19, 79). The two enzymes (here designated ROCT and SOCT, respectively) are encoded by different genes, which were previously cloned in this laboratory (66). Several lines of evidence suggest that the chief function of ROCT is to confer phaseolotoxin tolerance in the producing strains. These strains grow normally in media lacking arginine, even when they produce phaseolotoxin at maximal rates (at 18°C). In contrast, bacteria such as *Escherichia coli* and *Salmonella typhimurium* when grown under similar conditions are inhibited by phaseolotoxin, and this inhibition

is reversed by citrulline or arginine (77). The ROCT is not found in nontoxigenic strains (Tox⁻) of *P. syringae* pv. phaseolicola (79). The production of ROCT and phaseolotoxin are coregulated by temperature (15, 53, 79), and in the toxigenic strain NPS3121, the ROCT structural gene (*argK* [56]) is physically linked to a cluster of genes (*tax*) that are required for phaseolotoxin production (65, 66). Furthermore, the *argK* gene is apparently absent from closely related pathovars of *P. syringae* that do not produce phaseolotoxin and imparts resistance to phaseolotoxin in *E. coli* (66). Finally, mutational inactivation of the *argK* gene in strain NPS3121 by insertion of the transposable element Tn5 leads to a temperature-conditional arginine-bradytrophic phenotype (67).

In the present study, we characterized the *argK* gene from strain NPS3121, identified the promoter region, examined its regulation, and investigated its transcriptional and translational products. On the basis of the predicted amino acid sequence comparisons of ROCT with other OCTs and certain features of the *argK* sequence, we discuss the structural basis of phaseolotoxin and octicide tolerance in ROCT and the probable origin of the gene. Additionally, we report the transfer and expression of *argK* in tobacco.

(Some aspects of this work have been presented in preliminary form [52, 60]).

MATERIALS AND METHODS

Media, enzymes, and chemicals. Luria broth (47) and King's B broth (KB) (37) served as complex media, the former for *E. coli* and *Agrobacterium tumefaciens* and the

* Corresponding author.

TABLE 1. Bacterial strains and plasmids

Strain, plasmid, or bacteriophage	Source, reference, or relevant properties ^a
<i>Escherichia coli</i> K-12	
HB101.....	F ⁻ <i>hdsS20</i> (<i>hdsR hsdM</i>) <i>recA13 thi leu proA2 lacY1 galK2 rpsL xyl-5 mtl-1 supE44</i> λ ⁻ (47)
DH5α.....	F ⁻ <i>endA1 hsdR17</i> (r _K ⁻ m _K ⁻) <i>supE44 thi recA1 gyrA</i> φ801 <i>lacZΔM15 relA1</i> Δ(<i>lac-proAB-argF</i>) λ ⁻ (47)
CB877.....	<i>lacZ</i> ⁻ Y ⁺ <i>galK rpsL phoA8 hsdR hsdM</i> ⁺ <i>thi ilv recA56</i> (74)
CB957.....	CB806(pCB303) (74)
NECO1300.....	Nal ^r derivative of N134 Δ(<i>gpt-lac</i>)5 <i>relA1 spoT1 thi-1 ΔargI</i> λ ⁻ (66)
JM101.....	Δ(<i>lac-proAB</i>) <i>thi gyrA96 endA1 hsdR17</i> (r _K ⁻ m _K ⁺) <i>relA1 supE44</i> λ ⁻ /F' <i>traD36 proAB lac^rZΔM15</i> (47)
C600.....	<i>thi leu arg-14 proA2 lacY1 galK2 rpsL xyl-5 mtl-1</i> (47)
<i>Pseudomonas syringae</i> pv. phaseolicola	
NPS3121.....	WT Rif ^r Tox ⁺ (65)
NPS4336.....	<i>tox-4336::Tn5</i> (65)
4419.....	WT Tox ⁺ , R. E. Mitchell (54)
<i>Agrobacterium tumefaciens</i> ASE.....	Cm ^r Km ^r , plant transformation strain; Monsanto Co., St. Louis, Mo.
Plasmids	
pRCP17.....	Tet ^r IncP1; pLAFR3 cosmid clone carrying <i>argK</i> and the <i>tox</i> gene cluster (66)
pRCP23.....	Amp ^r Kan ^r <i>oriV_{E1}</i> ; pUC8-0.5-kb <i>EcoRI argK::Tn5</i> fragment from pRCP17 (66)
pLAFR6.....	IncP1 <i>rbxRK2</i> ⁺ <i>repRK2</i> ⁺ <i>cos</i> ⁺ Tet ^r ; broad-host-range vector carrying the multilinker of pUC18 flanking by synthetic <i>trp</i> terminators (25)
pCB303.....	Tet ^r IncP1; pRK290 derivative with a multilinker sequence sandwiched between divergently oriented promoterless <i>lacZ</i> and <i>phoA</i> (74)
pRK2013.....	<i>rep_{E1}</i> ⁺ Δ <i>rep_{RK2}</i> <i>tra_{RK2}</i> ⁺ <i>rbx_{RK2}</i> ⁺ Kan ^r (14)
pGEM5-Zf(+)	Amp ^r <i>lacZα oriV_{E1} oriV_{ts}</i> ; carries promoters for the T7 and SP6 polymerases facing toward the multilinker (Promega, Madison, Wis.)
pGEM7-Zf(+)	As above but with a different multilinker (Promega, Madison, Wis.)
pJIT117.....	Carries the <i>pea rbcS</i> transit peptide region between two tandem CaMV promoters upstream and the CaMV poly(A) addition signal downstream (26)
pGA482.....	Ti-derived transformation vector (2); Pharmacia-LKB
M13mp18, M13mp19.....	Sequencing vectors (50)

^a Nal^r, nalidixic acid resistant; WT, wild type; Rif^r, rifampin resistant; Cm^r, chloramphenicol resistant; Km^r, Kan^r, kanamycin resistant; Tet^r, tetracycline resistant; Amp^r, ampicillin resistant; CaMV, cauliflower mosaic virus.

latter for *P. syringae* pv. phaseolicola. The KB medium was prepared without MgSO₄, which was filter sterilized and added separately after autoclaving. The minimal glucose medium (MM) described previously (65) was supplemented with amino acids and vitamins required by various strains at the concentrations stated by Davis et al. (9). β-Galactosidase indicator agar plates were prepared as described in reference 47. Except as noted otherwise, the growth temperatures for *P. syringae* pv. phaseolicola and *A. tumefaciens* strains were 28 to 30°C, and that for *E. coli* strains was 37°C.

Restriction endonucleases, DNA polymerases, or other nucleic acid-modifying enzymes (Promega, Madison, Wis.), substrates, and chemical reagents for enzyme assays (Sigma Chemical Co., St. Louis, Mo.) were used as recommended by their respective suppliers or in the relevant publications.

Bacterial strains and plasmids. The bacterial strains and plasmids used are described in Table 1. Plasmid pRCP17 (66) served as a source of a 3.2-kb *HindIII-PvuII* fragment that carried the *argK* gene from *P. syringae* pv. phaseolicola NPS3121. Various plasmids used in functional studies are shown in Fig. 1 and were constructed as follows.

(i) **pEH1.** The 3.2-kb *PvuII-HindIII* fragment from pRCP17 carrying *argK* was initially cloned in pGEM7-Zf(+), that had been digested with *SmaI* plus *HindIII* in the orientations shown in Fig. 1, along with the restriction map of the 3.2-kb insert.

(ii) **pEH2.** The pEH1 plasmid was digested with *BstXI*, the ends were filled in with T4 DNA polymerase, and the DNA

was digested with *XhoI*, producing a 2.8-kb fragment that was isolated and ligated to the pGEM5-Zf(+) vector that had been digested with *EcoRV* plus *SaII*. This procedure inverted the orientation of *argK* relative to the *lac* promoter in the vector, compared with pEH1.

(iii) **pEH1.1 and pEH1.2.** pEH1 plasmid DNA was digested separately with *SacI* and *SphI* and recircularized to produce plasmids pEH1.1 and pEH1.2, respectively.

(iv) **pExo1, pExo2, pExo3, and pExo4.** These plasmids carry nested deletions into the insert of pEH1, produced after digestion with *ApaI* and *XbaI* and then exonuclease III treatment by using the Erase-a-Base system (Promega) according to the supplier's recommendations.

(v) **pEH3.** pEH1 was cleaved with *SmaI* and *EcoRI* (a *SmaI* site is present in the pLAFR3 multilinker carried over from pRCP17), and the digestion products were ligated to similarly digested pGEM7-Zf(+).

(vi) **pEH3.1 and pEH3.2.** Both plasmids are pEH3 derivatives with defined deletions of different segments. The first was obtained after digestion with *BalI* plus *EcoRI*, treatment with Klenow DNA polymerase, and recircularization, and the second was obtained after digestion with *SphI* and recircularization.

(vii) **pEH4 and pEH4.1.** Digestion of pEH1 with *EcoRI* or *SacI* and religation yielded plasmids pEH4 and pEH4.1, respectively.

(viii) **mp19.1 and mp19.2.** The 0.8- and 0.7-kb *XhoI-EcoRI* junction fragments from pRCP23 were cloned separately into

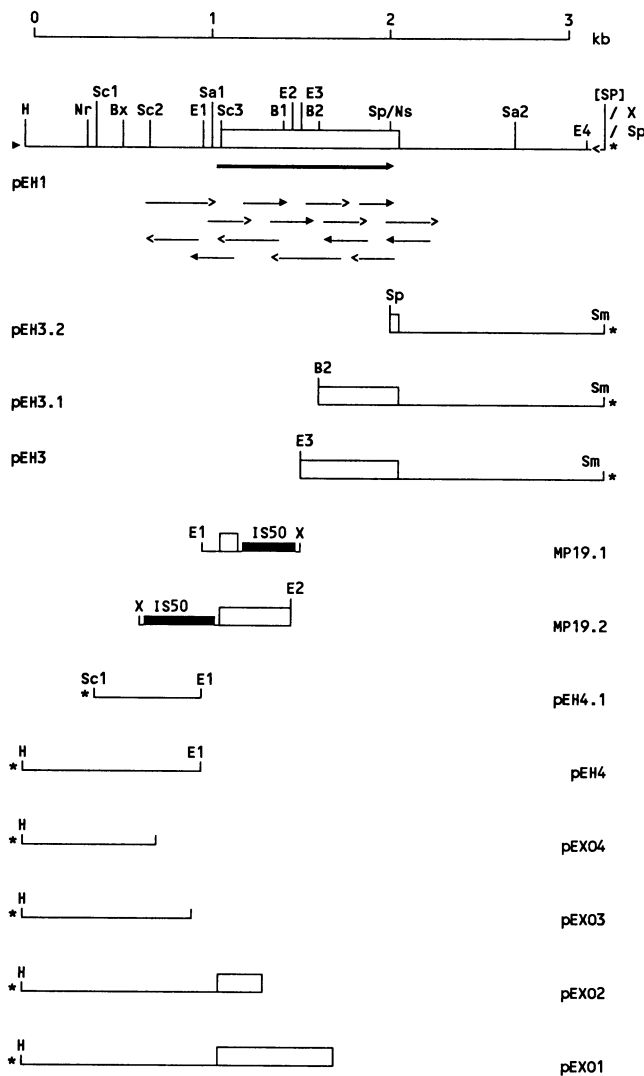


FIG. 1. Top to bottom: scale, physical map of the 3.2-kb *argK*-containing fragment in plasmid pEH1, position and orientation of sequencing primers ($5' \rightarrow 3'$, short arrows), and subclones and deletions used for the sequencing of *argK*. Restriction sites are abbreviated as follows: H, *Hind*III; Nr, *Nru*I; Ns, *Nsi*I; Sc, *Sac*I; Bx, *Bst*XI; E, *Eco*RI; Sm, *Sma*I; Sp, *Sph*I; Sa, *Sal*I; [SP]; *Sph*I-*Pst*I fusion site; X, *Xho*I. Multiple *Sac*I and *Eco*RI sites are numbered beginning from the left and are shown only in pEH1. Arrows with a solid head cover regions that were sequenced with the primers given in Table 2. Regions corresponding to the ROCT frame are shown as open rectangles. The direction of *argK* transcription is shown by the double arrow below the ROCT frame in pEH1. The solid bars in mp19.1 and mp19.2 correspond to terminal IS50 segments of Tn5 (see text). Asterisks mark the location of the Sp6 promoter in the pGEM vectors. Solid and line arrowheads at the left and right ends, respectively of the pEH1 insert mark the *lac* promoter in pGEM7-Zf(+) and pRCP17, respectively.

the synonymous sites of M13mp19 replicative-form molecules (50) and transformed into JM101 to produce mp19.1 and mp19.2, respectively. These derivatives provided the probes used in determining the exact position of a Tn5 insertion which leads to loss of *argK* function in pRCP17-T.1 (67), from which the pRCP23 insert originated.

(ix) **pEH10.** The ca. 1.6-kb *Sal*I fragment from pEH1 was

ligated to *Xho*I-linearized pGEM7-Zf(+) vector in the orientation shown in Fig. 1.

(x) **pEHL10.** The pEH10 DNA was digested with *Xba*I and *Hind*III (unique restriction sites in multilinker) and was ligated to the vector pLAFR6 that had been digested with the same two enzymes.

(xi) **pEHCB5.** Plasmid pEH1 was digested with *Eco*RI, filled in with Klenow DNA polymerase, and redigested with *Sal*I. The double digest was ligated to *Sma*I-*Xho*I-digested pGEM7-Zf(+) DNA. A plasmid containing the 0.48-kb *Sal*I-*Eco*RI fragment (pEH5) was identified by restriction enzyme analysis. This treatment was necessary to invert the orientation of the fragment relative to the *Xba*I and *Bam*HI sites on the vector's multilinker. The 0.48-kb insert was excised from pEH5 by digestion with *Xba*I plus *Bam*HI and ligated to similarly digested DNA of the promoter probe vector pCB303 (74) to produce pEHCB5. The direction of *argK* transcription in this plasmid is the same as that of the *phoA* gene on the vector. The plasmid was transferred to the *phoA* strain CB877 and to NPS3121 by pRK2013-assisted mobilization (14).

(xii) **pEHCB6.1.** A derivative of pEH1 lacking sequences to the right of the *Eco*RI₂ site within the *argK* coding region was initially made by partially digesting the plasmid with *Eco*RI and religating. The resulting plasmid (pEH6) was digested with *Nru*I plus *Mlu*I, the *Mlu*I ends were filled in with Klenow DNA polymerase, and the plasmid was recircularized to produce pEH6.1. A ca. 1.1-kb *Nsi*I-*Xba*I fragment containing the putative *argK* promoter region was excised from this plasmid and ligated to pCB303 that had been digested with *Pst*I and *Xba*I to produce plasmid pEHCB6.1. The direction of *argK* transcription in this plasmid is the same as that of the *phoA* gene of pCB303. *E. coli* DH5 α (pEHCB6.1) was used as the donor to transfer the plasmid to NPS3121 and CB877 by pRK2013-assisted mobilization (14).

(xiii) **pEH50 and pEH60.** Plasmid pEH1.1 was digested with *Sac*I, treated with T4 DNA polymerase in the absence of nucleotide triphosphates to trim the 3' overhangs, and cleaved with *Sal*I. These steps generated a ca. 1.5-kb fragment extending from a blunt end 10 nucleotides upstream of the putative translation initiation codon to a *Sal*I site about 0.5 kb downstream from the *argK* reading frame. Plasmid pJIT117 was digested with *Sph*I, treated with T4 DNA polymerase in the presence of dGTP to remove the three terminal nucleotides from the *Sph*I 3'-protruding ends, and cleaved with *Sal*I. These modifications allowed the directional cloning of the 1.5-kb *argK*-containing fragment into the pJIT117 multilinker and the fusion of the *rbcS* transit peptide and *argK* reading frames. The resulting plasmid, pEH50, was cleaved with *Kpn*I to release the 3.8-kb fragment that comprised the two cauliflower mosaic virus 35S promoters, the fused *rbcS* transit peptide-*argK* segments, and the viral polyadenylation signal. This fragment was cloned into the *Kpn*I site of the pGA482 multilinker to produce plasmid pEH60.

DNA sequencing. The dideoxy-chain termination method (70) was used for DNA sequencing. The labeled nucleotide was α -³⁵S-dATP (Amersham Corp., Arlington Heights, Ill.), and the products were separated on 4 or 6% denaturing pH gradient polyacrylamide gels (69). Double-stranded plasmid DNA templates were denatured (11) and sequenced by using the Sequenase kit (United States Biochemical Corp., Cleveland, Ohio) as recommended by the supplier. Each strand was sequenced with both dGTP- and dITP-containing reaction mixtures. Preparation of single-stranded templates of

TABLE 2. Oligonucleotide primers used in sequencing

Primer	Sequence	Position ^a
K1	5'-CAAGCCTGAAAAACCGC-3'	153-170
K2	5'-CCCGGCAGACAATATTCG-3'	381-399
K3	5'-TGGGTGAATCAGTCTCGG-3'	858-875
K4	5'-TATGGTGTCCGGCCTTGC-3'	957-941
K5 ^b	5'-GGCGGATCAATGAGGTGG-3'	231-212
K7	5'-GGCACAGATAAACAGCG-3'	1,269-1,253

^a Positions are relative to the *argK* transcription start point.

^b This primer was also used in the primer extension analysis.

the M13mp19 clones, denaturation, labeling, and termination reactions were done as described previously (50). The universal M13 primer (5'-GTAAAACGACGGCCAGT-3') and the -40 forward (5'-GTTTTCCAGTCACGAC-3') and reverse (5'-AACAGCTATGACCATG-3') primers were purchased from United States Biochemical Corp. Additional synthetic primers are shown in Table 2.

Molecular and genetic techniques. Standard molecular techniques were as described previously (47, 51). Bacterial RNA was isolated by the method of Gilman (21), and contaminating DNA was removed by treatment with RNase-free DNase I (Promega). Total RNA extracts from leaves of transgenic and control plants were prepared as described previously (90). Northern (RNA) hybridizations were performed by the method of Church and Gilbert (6), except that the hybridization and wash temperature was 78°C. Primer extension experiments were done by the method of Kingston (38) by using the K5 primer (Table 2). In vitro transcription of fragments cloned in pGEM5-Zf(+) and pGEM7-Zf(+) recombinant plasmids was done with Sp6 and T7 polymerases (Promega) as recommended by the supplier. The prokaryotic in vitro translation (Amersham) was used according to the supplier's instructions. Polypeptides produced by recombinant plasmids were labeled with [³⁵S]methionine (Amersham) and analyzed by electrophoresis in 11% denaturing polyacrylamide gels (45).

Functional and enzyme assays. The functionality of OCT encoded by various plasmids was tested in vivo by complementation of *E. coli* NECO1300 to arginine independence (66). Toxin production and toxin resistance in bacteria were obtained as described previously (65, 78). Alkaline phosphatase assays (49) were done without phenylmethylsulfonyl fluoride in the buffer used to wash the cells. Enzyme-specific activity was calculated by the method of reference 5. OCT activity in crude extracts from leaves of transgenic and control plants was assayed essentially as described in reference 63, using different ornithine concentrations, 25 min of incubation at 37°C, and final concentrations of 10 to 20 µg of total protein per ml and 0.47 to 2.7 µM phaseolotoxin in the filtrate. The amounts of substrates consumed in the reaction were less than 2%. Control reactions were done in the absence of either substrate or toxin extract. OCT activity units (micromoles of citrulline per minute per milligram of protein) were calculated using as reference a citrulline concentration standard curve.

Preparation of total protein extracts from leaves. Since purified tobacco OCT is unstable (18), OCT activity was determined in partially purified total protein extracts. Approximately 1.5 g of leaf tissue was homogenized in liquid nitrogen in the presence of 2.5 ml of homogenization buffer (100 mM Tris-HCl [pH 8.0], 50 mM ornithine, 5.0 mM EDTA, 50 mM K₂HPO₄, 5 mM β-mercaptoethanol) per g (fresh weight), sonicated in a Heat Systems-Ultrasonics,

Inc., model 350 sonicator at 30% duty cycle for 30 s at 4°C, and centrifuged for 20 min at 4°C in an SS34 Sorvall rotor at 10 krpm. The supernatant was passed through a sterile 0.45-µm-pore-size filter (Millipore Corp.), and proteins were precipitated at -20°C by adding 5 volumes of cold acetone. The precipitate was collected by low-speed centrifugation and resuspended in assay buffer (0.6 ml/g [fresh weight]) consisting of 10 mM Tris-HCl (pH 8.0), 1% (vol/vol) Triton X-100, 1 mM β-mercaptoethanol, and 10% (vol/vol) glycerol. The OCT activity in the extract remained stable during storage at -20°C and 50% final glycerol concentration. Bradford assays of protein concentration (4) included bovine serum albumin as a standard.

Phaseolotoxin-containing and control filtrates. The toxin-producing strains 4419 and NPS3121 were grown overnight in MM at 20°C. Sterile culture filtrates (0.45-µm-pore-size filter) were used as a source of toxin. A similarly prepared filtrate from the *tox* mutant NPS4336 was used as the control. The toxin concentration was determined by the *E. coli* bioassay (79) and was stable on storage in the dark at -20°C.

Plant transformation and crosses. Plasmid pEH60 was transferred into *A. tumefaciens* ASE by triparental mating (14). Aseptically grown *Nicotiana tabacum* 'Havana' SR1 plants were used as the source of leaf disks, and transformation was done by the method of Deblaere et al. (10). The media were supplemented with 200 µg of kanamycin per ml and when necessary with 500 µg of cefotaxime per ml. Some untransformed disks were allowed to regenerate plants without kanamycin selection (controls). Chlorosis assays were done by the leaf puncture method (54). Crosses were performed by transferring anthers from SR1 transformants that expressed *argK* RNA and ROCT activity to immature flowers of Glurk plants.

Nucleotide sequence accession numbers. The nucleotide sequences of *argK* and *argF* have been deposited with GenBank and assigned accession numbers M90049 and M99382, respectively.

RESULTS

Localization and sequencing of the *argK* region and identification of its polypeptide product. Hybridization of plasmid pRCP17 DNA with a mixture of the *Eco*RI-*Xho*I inserts carried in mp19.1 and mp19.2 indicated that the *argK* gene was localized in the 3.2-kb *Hind*III-*Pvu*II fragment, which includes 0.15 kb from the *lac* promoter region of pLAFR3. The exact position and the functional length of *argK* in this fragment were subsequently established by functional complementation tests done in the OCT-deficient *E. coli* NECO1300, using plasmids pEH1, pEH1.1, pEH1.2, pEH2, pEH10, and pEHL10 (Fig. 1 and 2). Plasmids pEH1.2 and pEHL10 were functionally inactive in these tests, while pEH1, pEH1.1, pEH2, and pEH10 fully complemented the indicator strain. Furthermore, pEH1 imparted on strain HB101 phaseolotoxin resistance (the other complementing plasmids were not tested in this regard). The functional difference between pEH10 and pEHL10 was attributed to the fact that pLAFR6 (the vector in pEHL10) contains synthetic *trp* terminators bracketing the multilinker sites. Taken together, the above results suggested that (i) the *argK* coding region has one of its borders near the *Sac*I₃ site and the other between the *Sph*I and *Sal*I₂ sites; (ii) the 1.6-kb *Sal*I fragment does not contain a functional promoter, although it carries an otherwise functional *argK* gene; (iii) plasmids pEH10 and pEH1.1 probably expressed *argK* from the *lac*

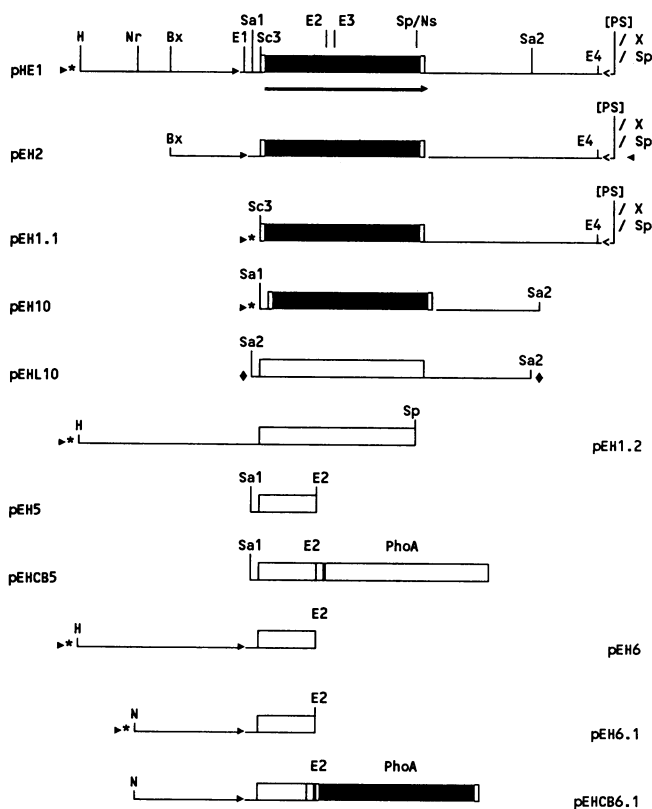


FIG. 2. Plasmids used for complementation analysis (pEH1, pEH2, pEH1.1, pEH10, and pEHL10) and for the construction of *argK-phaA* fusions (only the inserts are shown). Restriction sites, asterisks, and line arrowheads are as described in the legend to Fig. 1. The solid arrowheads outside the insert borders mark the location and direction of the *lac* promoter in the pGEM vectors, and those to the left of the ROCT frame indicate the location of the *argK* promoter. The ROCT frame in the plasmids able or unable to complement the OCT deficiency in *E. coli* NECO1300 is highlighted as solid or open rectangles, respectively. Diamonds show the synthetic *trp* terminators in pLAFR6.

promoter in the pGEM7-Zf(+) vector; and (iv) the *argK* promoter region spans the *SacI*₃-*SalI*₂ segment.

Nucleotide sequence of *argK* and identification of its product. A 1.3-kb segment that includes the *argK* gene plus limited portions flanking the ROCT-coding region was sequenced in both directions by the strategy shown in Fig. 1. Sequencing into the inserts of plasmids pEH4.1, pEH3, pEH3.1, and pEH3.2 and in the direction of the oligonucleotide primers K1, K2, and K3 (Table 2) covered the coding strand. In addition, clone mp19.1 was used to sequence the same strand across the putative ATG codon and to locate the position of the Tn5 insertion in pRC17.T-1 (Fig. 3). The noncoding strand was sequenced with the oligonucleotides K5, K4, and K7 (Table 2), the exonuclease III deletion derivatives of pEH1, bacteriophage mp19.2, and plasmid pEH1.2 (Fig. 1; see Materials and Methods).

The longest open reading frame present in the 1.3-kb segment spans 327 codons, starting with an ATG codon at positions +125 to +128 from the transcription start point (taken as +1, Fig. 3; see Fig. 6; see below). This frame has a 49.4% G+C content and is predicted to code for a 36.5-kDa polypeptide. A single protein band with an apparent molecular mass of ≈38 kDa was detected after in vitro transcrip-

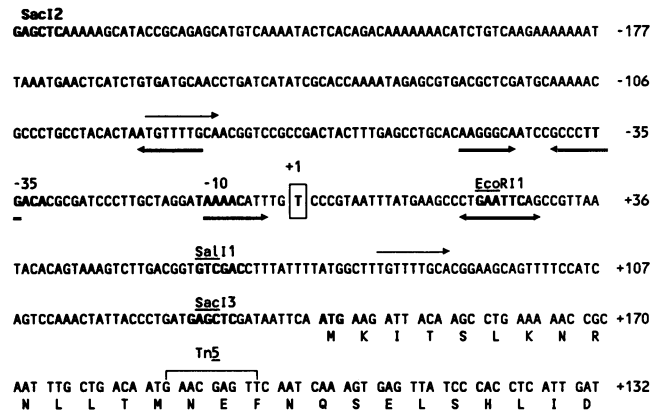


FIG. 3. Sequence of the promoter and N-terminal region of *argK*. The transcription initiation point (+1) is boxed. Thin and thick arrows mark the locations of the longest direct and inverted repeats, respectively, upstream from the ROCT frame. Pairs of corresponding repeats bear the same number, indicating their length. P designates a 10-bp perfect palindrome. The N-terminal amino acids of ROCT are shown in the one-letter code. The 9-bp duplication at the site of the Tn5 insertion in plasmid pRC17.T-1 extends from nucleotides +185 to +193. Restriction sites are designated as in the legend to Fig. 1.

tion-translation of plasmid pEH1 and then denaturing polyacrylamide gel electrophoresis (Fig. 4). These values are in close agreement with the size of other prokaryotic OCTs and the reported molecular mass of 110 kDa for the native (presumably trimeric) form of the enzyme (34). The predicted amino acid sequence of the 327-residue polypeptide aligns well with those of other OCTs (Fig. 5, discussed below). The nucleotide sequence of *argK* is identical to the one recently published (56) from another *P. syringae* pv. phaseolicola strain, except for the following differences in the 5'-upstream region: an extra G residue at position -18, an additional C residue at -36, and an inversion of the T and G nucleotides at positions -33 and -34.

The putative start codon is preceded by a reasonably good Shine-Dalgarno region (AtGAGcT, capital letters indicating identity with the optimal Shine-Dalgarno motif). Alternative initiations codons (GTG, TTG, ATT) occur further upstream and after the transcriptional start point of the *argK* gene (discussed below). However, none of these is preceded by a better Shine-Dalgarno region than the above ATG codon,

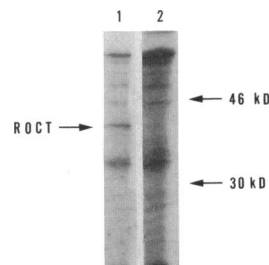


FIG. 4. Sodium dodecyl sulfate-polyacrylamide gel of in vitro translation products of plasmid pEH2 digested with *NdeI* and transcribed with T7 RNA polymerase (sense strand, lane 1) or digested with *NcoI* and transcribed with Sp6 RNA polymerase (antisense strand, lane 2). The position of the ROCT band is marked. kD, kilodaltons.

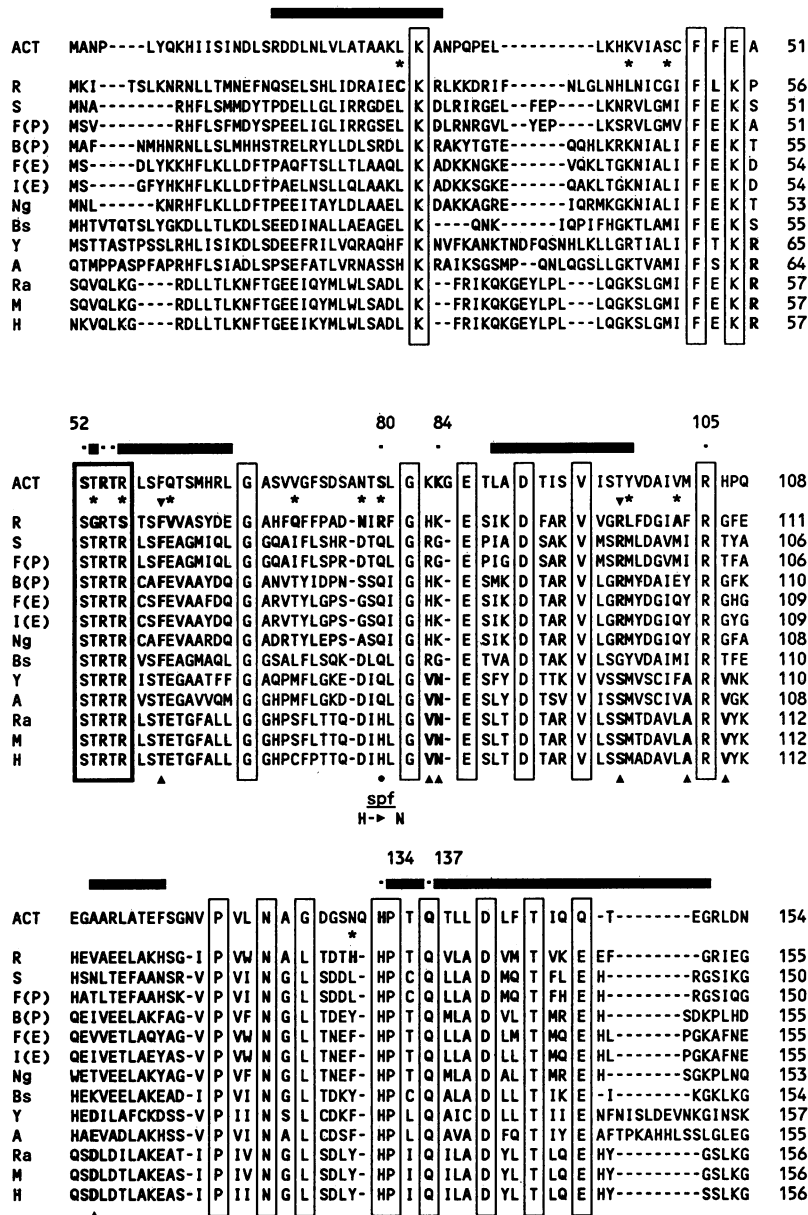


FIG. 5. Amino acid sequence alignments between ROCT and other prokaryotic and eukaryotic OCT sequences and the *E. coli* ACT (shown at the top). Residues in ACT and in the nonmitochondrial OCTs are numbered beginning with amino acid 2, according to the present usage (43, 91). Symbols: —, gaps; ★, positions where unique or unusual substitutions occur in ROCT; ▲, ▼, positions of unique residues in prokaryotic and eukaryotic OCTs, respectively; R, ROCT, and S, SOCT, both from *P. syringae* pv. phaseolicola (this study and reference 27, respectively); F(P) and B(P), anabolic and catabolic OCT, respectively, from *P. aeruginosa* (32, 84); F(E) and F(I), the ArgF and ArgI enzymes, respectively, of *E. coli* K-12 [88; the F(I) sequence is revised according to reference 43]; Ng, *N. gonorrhoeae* (48); Bs, *B. subtilis* (57); Y, *S. cerevisiae* (31); A, *A. nidulans* (86); Ra, rat (81); M, mouse (73); H, human (29). The *A. nidulans* and mammalian sequences are those of the mature peptide, as defined in the respective references (however, the number of residues indicated at the end of these sequences corresponds to the entire protein).

and all predict polypeptides with N termini substantially extended compared with those found among prokaryotic OCTs (Fig. 5). The ROCT frame is preceded by the hexanucleotides 5'-TTGACA-3' and 5'-TAaAAc-3', centered at positions -32 and -8, respectively, from the transcriptional start point, which match the -10 and -35 consensus hexanucleotides of canonical *E. coli* promoters at six and four positions, respectively. The putative -10 and -35 sequences suggested by other investigators (56) are not con-

sistent with the location of the transcription start point determined in our study. The -10 sequence also resembles closely that of the *Pseudomonas aeruginosa* *argF* gene encoding the anabolic OCT (TAtAAg [32]). However, the -35 motifs of the two genes match only at the first three positions. Two adjacent in-phase termination codons plus a third one located six nucleotides further downstream and a potential transcription termination structure (13-bp inverted repeat) follow the ROCT reading frame (not shown) at the

ACT	LHVAVMG	D	L	KYGR	TVHSL	Q	LAKFD	GNRF	YF	I	P	D	A	L	A	M	P	E	I	L	D	L	D	E	K	G	I	A	W	-----	S	L	H	S	S	I	E	216																		
R	VTIAYVG	D	G	NN	M	V	T	S	L	A	I	G	A	L	K	F	G	Y	N	L	R	I	I	A	P	-	N	A	L	H	P	T	A	V	L	A	G	I	E	Q	T	P	E	--	R	N	G	S	I	E	I	F	T	E	V	218
S	KTVAWIG	D	G	NN	M	C	N	S	I	E	A	A	I	Q	F	D	F	Q	L	R	V	A	C	P	-	A	G	Y	E	P	N	P	E	F	L	A	-----	G	E	R	V	T	I	V	R	D	P	205								
F(P)	KTVAWIG	D	G	NN	M	C	N	S	I	E	A	A	I	Q	F	D	F	Q	L	R	V	A	C	P	-	E	G	Y	E	P	K	A	E	F	V	A	-----	G	D	R	L	R	V	V	R	D	P	205								
B(P)	ISYAYLG	D	A	NN	M	G	N	S	L	L	I	G	A	L	G	M	D	V	R	I	A	A	P	-	K	A	L	W	H	D	E	F	V	A	Q	C	K	F	A	E	-----	S	G	A	K	L	T	L	T	E	D	P	218			
F(E)	MTLVYAG	D	A	NN	M	G	N	S	M	L	E	A	A	A	L	T	G	L	D	L	R	L	A	P	-	K	A	C	W	P	E	S	L	V	A	E	C	S	A	L	A	E	K	-----	H	G	G	I	T	L	T	E	D	V	218	
I(E)	MTLVYAG	D	A	NN	M	G	N	S	M	L	E	A	A	A	L	T	G	L	D	L	R	L	V	A	P	-	Q	A	C	W	P	E	A	A	L	V	T	E	C	R	A	L	A	Q	-----	N	G	G	I	T	L	T	E	D	V	218
Ng	TAFAYVG	D	A	Y	N	M	G	N	S	L	L	I	G	A	L	G	M	D	V	R	I	G	A	P	-	Q	S	L	W	P	S	E	G	I	A	A	A	A	A	A	K	E	-----	T	G	A	K	I	T	L	T	E	N	A	216	
Bs	VKVAYIG	D	G	NN	V	A	H	S	L	M	I	G	C	A	K	M	G	C	D	I	S	I	A	S	P	-	K	G	Y	E	V	L	D	E	A	E	A	A	K	T	A	L	Q	-----	S	G	S	V	T	L	T	D	D	P	216	
Y	LKMAWIG	D	A	NN	V	I	N	D	M	C	I	A	C	L	K	F	G	I	S	V	S	I	S	T	P	-	P	G	I	E	M	S	D	I	V	D	E	A	K	K	V	A	E	R	-----	N	G	A	T	F	E	L	T	H	S	215
A	LKIAWVG	D	A	NN	V	L	F	D	M	A	I	A	A	T	K	M	G	V	I	A	V	A	T	P	-	K	G	Y	E	I	P	P	H	L	E	I	K	S	A	G	E	V	S	K	P	K	L	L	Q	T	N	I	P	212		
Ra	LTLSWGID	D	G	NN	I	L	H	S	I	M	S	A	A	K	F	G	M	H	L	Q	A	A	T	P	-	K	G	Y	E	P	D	P	N	I	V	K	L	A	E	Y	A	K	E	-----	N	G	T	R	L	S	M	T	N	D	P	218
M	LTLSEWIR	D	G	NN	I	L	H	S	I	M	S	A	A	K	F	G	M	H	L	Q	A	A	T	P	-	K	G	Y	E	P	D	P	N	I	V	K	L	A	E	Y	A	K	E	-----	N	G	T	R	L	S	M	T	N	D	P	218
H	LTLSCFG	D	G	NN	I	L	H	S	I	M	S	A	A	K	F	G	M	H	L	Q	A	A	T	P	-	K	G	Y	E	P	D	A	S	V	T	K	L	A	E	Y	A	K	E	-----	N	G	T	K	L	L	T	N	D	P	218	

ACT	EVMAEVDILYM	TR	VQ	KER	LDPSEYANVKAQFV-L	R	ASDLHNAKANM	---K	V	L	H	H	L	P	L	-R	VD	271																		
R	AAGVHQADVIY	TD	W	I	SMG	ESVSV	EERIAL	LKPY	K	VTEK	M	A	L	T	G	K	A	D	-	T	I	F	M	H	C	L	P	A	F	H	D	-	278			
S	KAAVAGAHLYS	TD	W	T	SMG	QEEET	ARRNAL	FAPF	Q	V	T	R	A	S	L	D	L	A	E	K	D	-	V	L	F	M	H	C	L	P	A	H	R	G	E	265
F(P)	REAVAGAHLYS	TD	W	A	SMG	QEDEA	AARIAL	FRPY	Q	V	N	A	L	L	D	G	A	A	D	-	V	L	F	M	H	C	L	P	A	H	R	G	E	265		
B(P)	KEAVKGVDFVH	TD	W	V	SMG	EPVEAW	GERIKEL	LPY	Q	V	N	M	E	I	M	K	A	T	G	N	P	-	A	K	F	M	H	C	L	P	A	F	H	N	S	280
F(E)	VAGVKGADFIY	TD	W	V	SMG	EAKEK	WAERIAL	LRGY	Q	V	N	A	Q	M	A	L	T	D	N	P	-	V	K	F	L	H	C	L	P	A	F	H	D	280		
I(E)	VKGVEGADFIY	TD	W	V	SMG	EAKEK	WAERIAL	LRGY	Q	V	N	S	K	M	M	L	T	G	N	P	-	V	K	F	L	H	C	L	P	A	F	H	D	280		
Ng	HEAVKGVGFH	TD	W	V	SMG	EPKEV	QERID	LKDY	R	V	T	P	E	L	M	A	A	S	G	N	P	-	V	K	F	M	H	C	L	P	A	F	H	N	R	278
Bs	IEAVKDADVIY	SD	V	F	SMG	QEAE	QERL	AVFAPY	Q	V	N	A	L	V	S	H	A	K	P	D	-	Y	T	F	L	H	C	L	P	A	H	R	E	276		
Y	LKASTNANILV	TD	T	F	SMG	EEFAK	QAKL	QKFGF	Q	I	N	Q	E	L	V	S	A	D	P	N	-	Y	K	F	M	H	C	L	P	A	R	H	Q	E	272	
A	EEAVKDADILV	TD	T	W	SMG	QEEEK	AQRL	KEFDGF	Q	I	T	A	E	L	A	K	R	G	G	A	K	E	G	W	F	M	H	C	L	P	A	R	H	P	E	261
Ra	LEAARGGNVLI	TD	T	W	SMG	QEDEK	KKRL	QAFQGY	Q	V	T	M	K	T	A	K	V	A	A	S	D	-	W	T	F	L	H	C	L	P	A	R	K	P	E	277
M	LEAARGGNVLI	TD	T	W	SMG	QEDEK	KKRL	QAFQGY	Q	V	T	M	K	T	A	K	V	A	A	S	D	-	W	T	F	L	H	C	L	P	A	R	K	P	E	277
H	LEAARGGNVLI	TD	T	W	SMG	REEEK	KKRL	QAFQGY	Q	V	T	M	K	T	A	K	V	A	A	S	D	-	W	T	F	L	H	C	L	P	A	R	K	P	E	277

ACT	-----	E	I	A	T	D	V	D	K	T	P	H	A	Y	F	Q	Q	A	G	N	G	I	F	A	R	Q	A	L	L	V	N	R	D	L	V	L	*	310									
R	---LDTEVARETPDL---	V	E	V	E	S	V	F	E	G	P	Q	S	R	V	F	D	Q	G	E	N	R	M	H	T	I	K	A	L	M	L	E	T	V	V	P	*	326									
S	-----	E	I	S	V	D	L	L	D	S	R	S	V	A	N	D	Q	A	E	N	R	L	N	A	Q	K	A	L	L	E	F	L	V	A	P	S	H	O	R	A	*	305					
F(P)	-----	E	I	S	E	D	L	L	D	D	P	R	S	V	A	N	D	Q	A	E	N	R	L	N	A	Q	K	A	L	L	E	L	L	I	E	H	A	H	A	*	304						
B(P)	ETKVGKQIAEQPNLANGI	E	V	T	E	D	V	F	E	S	P	Y	N	I	A	F	E	Q	A	E	N	R	M	H	T	I	K	A	I	L	V	S	T	L	A	D	I	*	335								
F(E)	QTTLGKQMAKEF-DLHGGM	E	V	T	E	D	V	F	E	S	A	S	I	V	F	D	Q	A	E	N	R	M	H	T	I	K	A	V	M	M	A	T	L	G	E	*	333										
I(E)	QTTLGKQMAKEF-DLHGGM	E	V	T	E	D	V	F	E	S	A	S	I	V	F	D	Q	A	E	N	R	M	H	T	I	K	A	V	M	V	A	T	L	S	K	*	333										
Ng	ETKVGEWIYETF-GLN-GV	E	V	T	E	D	V	F	E	S	P	A	G	I	V	F	D	Q	A	E	N	R	M	H	T	I	K	A	V	M	V	A	L	G	D	*	330										
Bs	-----	E	V	T	A	E	I	D	G	P	N	S	A	V	F	Q	A	E	N	R	L	H	V	Q	K	A	L	K	A	I	L	Y	K	G	E	S	S	K	N	C	*	318					
Y	-----	E	V	S	D	D	V	F	Y	G	E	H	S	I	V	F	E	A	E	N	R	L	Y	A	A	M	S	A	I	D	I	F	V	N	K	G	N	F	K	D	L	K	*	338			
A	-----	E	V	S	D	E	V	F	Y	S	N	R	S	L	V	F	P	E	A	E	N	R	L	W	A	A	I	S	A	L	E	G	F	V	N	K	G	I	E	*	327						
Ra	-----	E	V	D	E	V	F	Y	S	P	R	S	L	V	F	P	E	A	E	N	R	K	W	T	I	M	A	V	M	V	S	L	L	T	D	Y	S	P	V	L	Q	K	P	K	F	*	322
M	-----	E	V	D	E	V	F	Y	S	P	R	S	L	V	F	P	E	A	E	N	R	K	W	T	I	M	A	M	V	S	L	L	T	D	Y	S	P	V	L	Q	K	P	K	F	*	322	
H	-----	E	V	D	E	V	F	Y	S	P	R	S	L	V	F	P	E	A	E	N	R	K	W	T	I	M	A	V	M	V	S	L	L	T	D	Y	S	P	V	L	Q	K	P	K	F	*	322

FIG. 5—Continued.

same positions as in the gene studied by Mosqueda et al. (56).

Similarity between ROCT and other OCTs. Optimized sequence alignments among 13 OCTs (8 bacterial, 2 fungal, and 3 mammalian) and ROCT were obtained with the program CLUSTAL (28) with minor visual adjustments that seemed to improve the alignment (Fig. 5). The ROCT has significant but, overall, low similarity to other OCTs (≈ 30 to $\approx 45\%$ identical amino acid residues

TABLE 3. G+C content of OCT-encoding genes and similarities between ROCT and other OCTs

Sequence	% G+C	% Identical residues ^a	
		Nucleotide	Amino acid
ROCT	49.4		
<i>P. aeruginosa</i> ArcB	63.1	56	42.8
<i>N. gonorrhoeae</i> ArgF	54.3	53.4	43.4
<i>E. coli</i> K-12 ArgF	58.6	52	44.9
<i>E. coli</i> K-12 ArgI	51.6	50	44.6
<i>P. syringae</i> pv. phaseolicola ArgF	57.3	44	35.6
<i>P. aeruginosa</i> ArgF	67.9	46	35.4
<i>B. subtilis</i> ArgF	48.4	64.2	35.4
<i>S. cerevisiae</i> ARG3	36.8		34.5
<i>A. nidulans</i> ArgB	53.5		30.2
Human	44.8		31.3
Mouse	44.8		30.4
Rat	45.8		30.7

^a Calculated on the basis of the alignments in Fig. 5.

presented in Fig. 5 revealed unique occupancies at several positions, which clearly distinguish the prokaryotic from the eukaryotic OCTs (Table 4). For example, the positions corresponding to residues 62, 232, and 315 of the *E. coli* ArgI enzyme have mutually exclusive occupancies (F, V, and Q residues, respectively, in the prokaryotic OCTs and T, V, and E residues in the eukaryotic enzymes). Position 274 in the ArgI sequence (A in the prokaryotic group and either a gap or R in the eukaryotic group in our alignment) essentially conforms to the above rule. Three additional occupancies in the prokaryotic (M, H, and K at positions 168, 321, and 324, respectively) and seven in the eukaryotic (P, V, N, A, V, T, and Y at positions 73, 85, 87, 105, 112, 187, and 306,

TABLE 4. Unique or unusual amino acid substitutions in ROCT^a

Residue in ROCT ^b	Position in <i>E. coli</i> ArgI	Occupancy in other OCTs
C-31	29	L, F, I
L-47	45	K, R
G-51	49	M, L
L-54	52	E, S, T
G-58	56	T
S-61	59	R
V-65	63	E
E-71	69	L, Q, F, M
Q-76	74	T, M, S, I, L
N-82	80	D, G, S, A
R-84	82	Q, H
F-94	92	T, S
L-101	99	M
H-134	133	F, Y, L
T-171	167	N, F, H
H-193	192	E, W
S-240	239	E, A, P
S-242	241	E, A
K-253	254	Q, R
S-297	304	E, D
R-305	312	I, L, V, A
G-309	317	A
E-323	330	A, S, G, I, F, L

^a Only substitutions at positions that are invariant, are occupied by the same residue in at least four OCT sequences (excluding ROCT), or involve residues of different chemical character are included.

^b Positions in ROCT are numbered from the second residue in line with present usage (43).

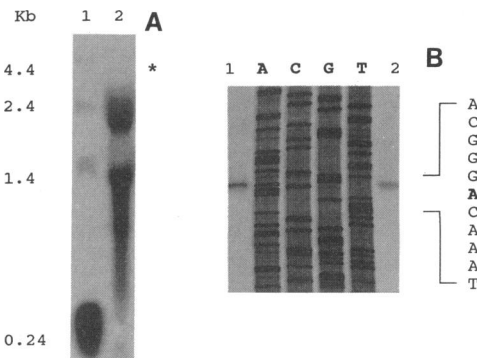


FIG. 6. Northern blot (A) and primer extension analysis (B) of *argK*. (A) Lane 1, ³²P-labeled RNA marker (Boehringer-Mannheim); lane 2, total RNA from strain NPS3121 grown in KB medium at 28°C hybridized to single-stranded (antisense) RNA probe (T7 transcript from pEH10 linearized with *Hind*III (see text). The asterisk indicates the position of a faint band of ~4 kb. (B) Lanes 1 and 2, total RNA from NPS3121 grown in KB medium at 28°C and MM at 21°C, respectively.

respectively) sequences show absolute invariance within their respective group but are not found in the other group. Finally, positions 98, 184, and 187 of the prokaryotic group (R or G, R or S, and R or S, respectively) and 112 (D or E) of the eukaryotic group have only single exceptions to the unique occupancy rule. These groups of residues may be considered kingdom-specific amino acid signatures for OCTs, and it is interesting that the ROCT bears the prokaryotic signature at all the above positions.

Figure 5 reveals the extensive conservation in primary structure between OCTs and highlights the unique or unusual substitutions in the ROCT suggested by our optimized alignments. Two unique substitutions occur in the highly conserved pentapeptide STRTR, as previously noted by Mosqueda et al. (56). Although both are evolutionarily conservative in character, they replace a hydroxyl-containing amino acid with one that lacks a side chain (G) and one having a basic side chain (R) with chemically dissimilar residue (S). There are three additional unique substitutions in ROCT (V-65, K-253, G-309), not revealed by the alignment of four prokaryotic OCTs published by these investigators (56), which replace universally conserved residues (E, Q, and A, respectively) in all other OCTs. Several additional substitutions of unusual character occur throughout the ROCT sequence (Table 4; Fig. 5). The A residue at position 130 (position 129 in our numbering system) noted as a unique substitution in ROCT by Mosqueda et al. (56) is not retained as a unique feature in the present alignment.

Location and regulation of an *argK* promoter. The complementation analysis with the plasmids depicted in Fig. 2 suggested that the *argK* promoter region lies within the 0.6-kb *Sac*I₁-*Sac*I₃ segment of the physical map shown in the figure. To verify the location of the *argK* promoter and analyze its regulation, we subcloned the *Sal*I₁-*Eco*RI₂ and the *Nru*I-*Eco*RI₂ fragments in the broad-host-range promoter probe vector pCB303 (plasmids pEHCB5 and pEHCB6.1, respectively; Fig. 2). The first plasmid contains only a portion of the 0.6-kb *Sac*I₁-*Sac*I₃ fragment upstream of *phoA*, while the second contains the entire fragment. Comparison of the *phoA* activities expressed by pCHCB5 and pEHCB6.1 showed that the *Nru*I-*Eco*RI₂ fragment carries a promoter that is functional in *P. syringae* pv. phaseolicola.

TABLE 5. Activity of the *argK* promoter in *P. syringae* pv. phaseolicola NPS3121

Plasmid	Growth conditions		PhoA activity ^a (plasmid - control ^b)
	Medium	Temp (°C)	
pEHCB6.1	MM	21	49
	MM + arginine ^c		72
	MM	28	35
	MM + arginine		75
pEHCB5	MM	21	ND ^d
	MM + arginine	21	ND
	MM	24	ND
	MM + arginine		ND

^a Units are micromoles of citrulline formed per minute per milligram of protein.

^b Control cultures carried the vector plasmid pCB303.

^c Arginine concentration was 0.1%.

^d ND, no detectable activity above that of the control (NPS3121[pCB303]).

cola (Table 5) as well as in *E. coli* CB877 (data not shown), while the *SaII*₃-*EcoRI*₂ fragment lacked promoter activity. These results confirm the location of the *argK* promoter deduced from our complementation analysis.

Previous studies done with different strains of *P. syringae* pv. phaseolicola (19, 33, 79, 82) showed that growth temperature modulates the level of ROCT specific activity, which decreases as the growth temperature is raised from 18 to 30°C. Templeton et al. (83) further showed that arginine, which causes repression of anabolic OCTs in most microorganisms, did not have a significant effect on the specific activity of ROCT from *P. syringae* pv. phaseolicola 4419. To determine the possible effects of growth temperature and arginine on *argK* promoter activity, we quantified the level of *phoA* expression in strain NPS3121(pEHCB6.1) grown at two different temperatures (21 and 28°C) in MM with and without arginine (0.1%). Cultures grown at 21°C without arginine supplementation expressed 40% higher PhoA activity than those grown at 28°C. Thus, the lower ROCT activity at the higher temperatures reported in earlier studies (33) is partially reflected in decreased *argK* transcription. However, in medium supplemented with 0.1% arginine, the PhoA activities were essentially equal at the two temperatures and both were significantly higher than the activities measured in nonsupplemented medium. Therefore, it appears that arginine increases *argK* transcription and cancels the thermoregulation of the *argK* promoter.

***argK* transcripts.** The size and number of ROCT transcripts were analyzed by Northern blot hybridization of total RNA separated on denaturing gels with three different probes. Initially, the 0.96-kb *SacI*-*SphI* fragment purified from agarose was used as a probe, and three different mRNA species were detected, having sizes of about 1.2, 2.3, and 4 kb (Fig. 6A). Hybridization with single-stranded RNA probes of opposite polarity to the ROCT frame, produced by in vitro transcription from plasmid pEH10, revealed three transcripts of the size as those detected with the double-stranded probe, while a probe with the same polarity as the ROCT frame did not produce any signal. All three transcripts were present in cultures grown in MM at 21°C and in KB medium at 28°C. The shorter transcript had the size expected of a monocistronic ROCT message. The double-stranded DNA probe used terminates before the putative ROCT translational stop codon and extends 12 nucleotides upstream of the putative *argK* initiation codon. Therefore,

the two larger transcripts do not initiate downstream from the ROCT frame and either terminate in the 70-bp *SaII*₁-*SacI*₃ segment or transverse the ROCT coding region, wholly or in part.

To further characterize *argK* transcription, we performed primer extension analysis using the oligonucleotide K5 as a primer. A single transcription start point was identified (T, Fig. 6B) which is located 143 nucleotides upstream from the putative translation initiation codon. Changing the growth temperature and medium complexity (21°C in MM and 28°C in KB medium) did not alter the point of transcription initiation. Taken together, the Northern blot and primer extension analyses suggest that ROCT is translated from more than one mRNA, at least one of which initiates close to the putative ATG codon. The other two transcripts may initiate at the same position or at other locations, either further upstream or within the ROCT frame.

Transformation, functional expression of ROCT, and chlorosis resistance in tobacco. The functional expression of ROCT in plants would provide an important new tool to investigate the pathophysiological consequences of phaseolotoxin action in plants and evaluate the possibility for germ plasm improvement in bean. To explore these possibilities, we introduced the *argK* gene into *N. tabacum* 'Havana' SR1 by *Agrobacterium*-mediated transformation. Previous studies (12, 16, 22) suggested that plant OCTs are present in several subcellular compartments, one of which, the chloroplast, is the most likely cellular target of phaseolotoxin (53, 85). Accordingly, we constructed plasmid pEH60 (Fig. 7) to enable the ROCT protein to enter into the chloroplasts. The chimeric protein retained biological activity, i.e., it complemented *E. coli* NECO1300 to arginine prototrophy and was resistant to phaseolotoxin in vitro (Table 6). Total RNA from 23 regenerated kanamycin-resistant (Km^r) transformants was examined for the presence of *argK*-specific mRNA by Northern blot hybridization after denaturing gel electrophoresis. The probe consisted of the antisense transcript produced by the T7 polymerase from plasmid pEH6.1 that had been linearized by cleavage with *NsiI* (Fig. 2). Five transformants contained a distinct band that hybridized strongly to the probe (Fig. 8). The apparent size of this transcript was about 2.0 kb, which is consistent with the coding size of the chimeric *rbcsS::argK* fusion in pEH60. This transcript was not present in total leaf RNA extracts derived from control 'Havana' SR1 or untransformed Turkish and Glurk tobacco.

The presence of functional ROCT protein in plants was investigated by comparing the specific activity of OCT in total protein extracts from leaves of SR1 transformants expressing *argK* RNA in the presence and absence of phaseolotoxin. Additionally, several F₁ progeny from the cross between the transformant II-3.2 and Glurk tobacco were similarly analyzed. Two groups of plants could be distinguished (Table 6). Group I plants had OCT activity that was virtually resistant to phaseolotoxin (plants 21-A, II-2.3, 4393, and another F₁ progeny, not shown); group II plants had OCT activity that had moderate or no detectable resistance to the toxin (plants 24 and II-4.1, respectively, and two others not shown). The degree of resistance in OCT from the group I plants was comparable to that of the OCT encoded by plasmid pEH50 (0 to 17% inhibition), while the degree of sensitivity of the OCTs in group II plants was comparable to that of the untransformed controls (SR1 or Glurk, 53 to 73 and 78% inhibition, respectively). The greater degree of resistance of the in vitro OCT activity in group I plants seemed to correlate with a higher level of total OCT specific activity (135 to 183% higher than the controls).

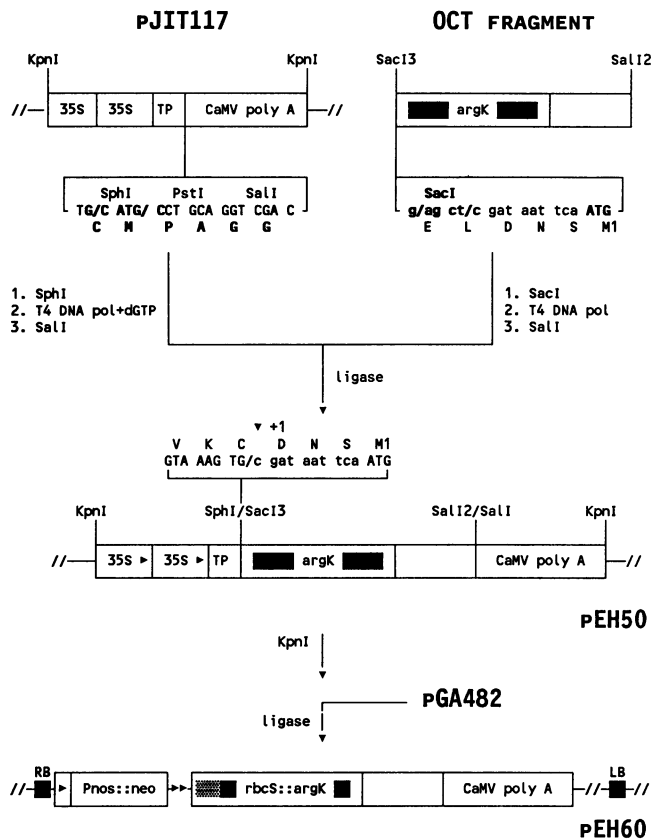


FIG. 7. Construction of plasmid pEH60. Plasmid pJIT117 (26) carries the chloroplast transit peptide region (TP, ) of *rbcS* from pea and two tandem copies of the 35S promoter (35S) and the poly(A) addition signal region (poly A) from the cauliflower mosaic virus (CaMV). The *argK* fragment extends from the *SacI*3 site just upstream from the putative ATG codon of ROCT to about 0.6 kb past the gene's termination codon. The in-frame fusion in pEH50 carries the RbcS transit peptide up to the cysteine residue preceding the cleavage site and is followed by aspartate, asparagine, and serine residues encoded by the *SacI*3-ATG segment of *argK* which are not present in the predicted ROCT peptide. The amino acid sequence generated at the fusion point conforms to the consensus transit peptide cleavage site of chloroplast proteins (20). pol, polymerase.

Since the pH activity profile can often serve as a means for identification of particular enzyme isoforms and to further characterize the OCTs in the transformed plants, we determined and compared these profiles in protein extracts from a group I transformant (21A), untransformed SR1, and *E. coli* NECO1300(pEH1) in the pH range from 8.0 to 9.5. The activity profile from plant 21A (Fig. 9) clearly differs both from that of the control plant and from that of the bacterial extracts, demonstrating that this plant expressed an additional OCT compared with the control. The profiles shown in Fig. 9 are from one of three experiments which gave essentially similar results.

The physiological significance of the toxin-tolerant OCT activity found in the transgenic plants was tested by applying toxin-containing culture filtrates to leaves. Because the development of chlorosis by locally applied toxin depends both on the developmental stage of the leaf and on environmental factors, the assays were done on leaves at different developmental stages, both in a growth chamber and in the greenhouse. Toxin-containing and toxin-lacking filtrates

TABLE 6. OCT activity in leaves of 'Havana' SR1 and Glurk tobacco, in *rbcS-argK* transformants of SR1, and in F₁ progeny of a Glurk × II-2.3 cross

Enzyme source	OCT sp act ^a		% Inhibition ^b	
	No toxin ^c	Plus toxin ^d	Actual	Avg
SR1 control	0.101 0.088	0.047 0.024	53 73	60 (10)
SR1 transformant				
21A	0.322 0.235	0.342 0.207	0 12	8 (4)
II-2.3	0.164 0.158	0.141 0.133	14 16	15 (4)
II-4.1	0.053 0.043	0.023 0.014	57 67	62 (2)
24	0.100 0.108	0.062 0.055	38 49	44 (2)
Glurk control	0.080 0.081	0.018 0.019	78 77	78 (2)
F ₁ Glurk × SR1 (4393)	0.118 0.201	0.116 0.191	2 5	4 (2)
NECO1300(pEH50)	0.003 0.006	0.003 0.005	0 17	8 (6)

^a Units were micromoles per minute per milligram of protein.

^b Numbers in parentheses indicate the number of experiments on which the average inhibition values were calculated. All values have been rounded to the nearest decimal.

^c For each enzyme source, the values in the upper and lower lines are from experiments that gave the lowest and highest percent inhibition, respectively.

^d Toxin concentration was 2.7 μM; ornithine concentration was 2.5 mM.

with or without 0.3 mM citrulline or arginine were routinely assayed on the same leaf. Chlorosis was observed only with the toxin-containing filtrate lacking citrulline or arginine and was reproducible in leaves of Glurk and Turkish tobacco controls but less reproducible in untransformed SR1 plants. Chlorosis was never seen in transgenic SR1 leaves treated with the toxin-containing extracts.

DISCUSSION

Origin of the *argK* gene. The evolutionary origin of ROCT and its structural gene is of considerable interest in the context of plant pathogen evolution and tolerance to auto-toxic antibiotics in microorganisms (7, 15). The present study and data to be reported elsewhere (27) clearly establish that the enzyme did not evolve from the housekeeping SOCT. First, the nucleotide sequence of *argK* has the lowest

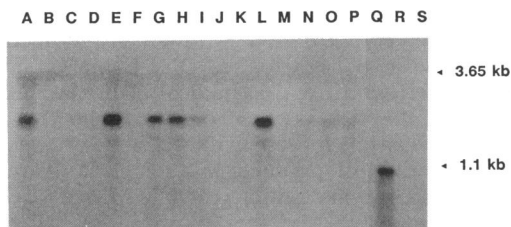


FIG. 8. Northern blot analysis of transgenic SR1 tobacco plants. Lanes: A to P, total RNA from independent transformants; Q, total RNA from NPS3121 as a positive control; R and S, total RNA from untransformed tobacco as negative controls.

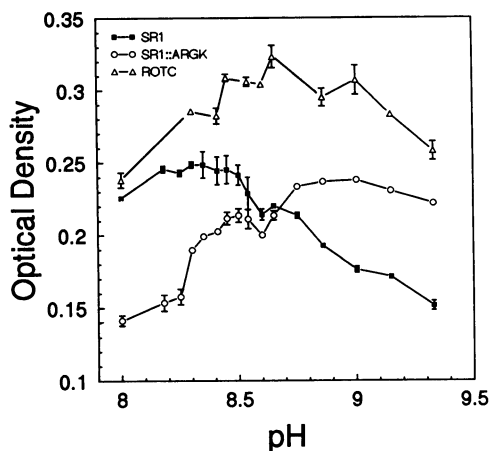


FIG. 9. Comparison of pH activity profiles of OCT in extracts that were prepared from untransformed tobacco 'Havana' SR1 (SR1), from transformant 21A (SR1-ArgK), and from *E. coli* NECO1300(pEH1) (ROCT). The activities were determined as described in Materials and Methods and by adjusting the pH of the assay buffer to the values shown. Each point is the average of triplicate assays (bars show the standard error).

similarity to the *argF* gene encoding the SOCT from the same strain (44% identity [27]) compared with other prokaryotic OCT-encoding genes, and the same applies to their respective proteins (35.6% identity). Second, the G+C content of *argK* (49.4% in the ROCT frame) is considerably lower than that of the *P. syringae* pv. phaseolicola genome (56% [75]), the *argF* gene (57.3% [27]), and several pathogenicity genes (*hrp*) from the same strain that have been sequenced (56 to 58% [25]). The G+C content of eubacterial protein-coding genes is typical of the organism's genomic G+C content, in contrast to that of nontranslated genes (specifying rRNAs or tRNAs), which is considerably lower (58, 71). This is consistent with the idea that *argK* was not derived from the *argF* gene of *P. syringae* pv. phaseolicola, but must have immigrated into organism's genome from another source. The kingdom-specific amino acid signatures identified in this study strongly suggest that *argK* originated from another prokaryote which may have been the original phaseolotoxin producer. This progenitor most likely had a low G+C content, which would exclude most fluorescent *Pseudomonas* spp. (13). The physical proximity of *argK* to the cluster of the genes involved in phaseolotoxin biosynthesis and its role in resistance argue that the entire *argK-tax* cluster was transferred together into the *P. syringae* pv. phaseolicola genome. Another probable case of interspecies transfer of an anabolic OCT gene exists, namely, the *E. coli argF* gene (87), for which a prokaryotic origin has also been proposed, based on similar argumentation. A probable mechanism for this transfer has been suggested based on the presence of insertion sequence elements on a 10-kb segment flanking *argF*, but no similar information exists for *argK* or the *argK-tax* gene cluster. The selective pressures which may have promoted this transfer are more obvious for *argK* than for the *E. coli argF* gene.

Since *argK* and *tax* gene homologs are absent from the genomes of closely related pathovars of *P. syringae* which do not produce phaseolotoxin (66, 67), it is simplest to assume that the genes entered *P. syringae* pv. phaseolicola after these pathovars radiated from their common ancestor. An approximate upper limit for the time when some of the

pathovars first existed as plant pathogens can be suggested, based on sequence comparisons of their common pathogenicity genes (*hrp*). By comparing the rate of synonymous substitutions in *hrp* gene sequences from *P. syringae* pv. phaseolicola, *P. syringae* pv. savastanoi, and *P. syringae* pv. glycinea (25), we estimated the time of separation of the *hrpS* gene homolog of *P. syringae* pv. phaseolicola, *P. syringae* pv. savastanoi, and *P. syringae* pv. glycinea to be ≈ 1 million years. Accordingly, the presumed introgression of *argK* into the *P. syringae* pv. phaseolicola genome probably took place in very recent evolutionary time, about 1 million years ago or less.

Conservation of primary structure and functional significance of unique substitutions in ROCT. The optimized sequence alignments shown in Fig. 5 highlight the extensive conservation in primary structure among OCTs, including ROCT. The positionally invariant amino acid residues and oligopeptide motifs amount to about 12% of the average polypeptide length. As noted by other investigators (30–32, 41–44, 84, 88), there is high conservation of primary structure between OCTs and the catalytically related aspartate transcarbamoylases (ACTs). The majority of invariant residues have not been implicated in substrate binding or catalysis in either OCT or ACT (30, 43, 72) and are presumably conserved for structural reasons. Beyond the overall similarity in its primary structure, ROCT has several unique amino acid substitutions relative to the other enzymes (Table 4). A definitive assessment of the functional significance of the several unique amino acid substitutions in the unusual kinetic properties (82, 83) and octicidine and phaseolotoxin tolerance of ROCT will ultimately require site-directed mutagenesis and knowledge of the three-dimensional structure of the enzyme and enzyme-ligand complex (24, 35, 36, 40, 80, 91). In the following paragraphs, we discuss the possible significance of these substitutions in the enzyme's intrinsic resistance to octicidine and phaseolotoxin.

As far as is presently known, ROCT is the only enzyme that is resistant to octicidine and phaseolotoxin. All 17 OCTs from plant and bacterial sources that have been tested in vitro and/or in vivo were sensitive to octicidine and phaseolotoxin (18). Of the enzymes whose sequences are available, the two OCTs from *E. coli* K-12, the enzyme from *S. typhimurium*, and the anabolic OCT from *P. aeruginosa* are also sensitive based on in vitro and/or in vivo assays (66, 77–79; this study, data not shown). The same applies to the housekeeping SOCT of *P. syringae* pv. phaseolicola (66). Additionally, the rat liver enzyme is presumed to be sensitive, based on early studies with toxin isolated from halo blight-diseased leaves that was thought to have a different chemical structure but, in light of current knowledge, was probably octicidine (53). Finally, the *S. cerevisiae* enzyme is assumed to be sensitive to octicidine since it is inhibited in vivo by δ -N-(phosphonacetyl)-L-ornithine (39) which is active against OCTs from diverse organisms but not against ROCT (79).

The primary and predicted secondary structures of the N-terminal half of OCT (up to about residue 150) are very similar to the "equatorial" (carbamoylphosphate [CP]-binding) domain of ACT (30, 31, 88, 92, and our own alignments). Thus, the stereochemical disposition of these residues in the active-site cleft of OCT is probably similar (although not necessarily identical) to that in ACT. The crystal structure of the *E. coli* ACT complexed with various ligands (24, 35, 36, 40, 80, 91, 93) indicates that the side chains of residues S-52, R-54, T-55, R-105, H-134, and Q-137 from one catalytic chain and of S-80 and K-84 from the adjacent catalytic chain

all interact with CP and phosphonacetyl aspartate. In one particular case, in which CP and succinate are present as ligands, the CP additionally interacts with the side chain of T-53 (24). Based on the alignments in Fig. 5 and on similar alignments published by others (32, 46, 56, 86, 92), the positionally correspondent residues in ROCT are S-57, G-58, R-59, T-60, R-108, H-135, Q-138, I-83, and K-88. Among the unique substitutions in ROCT are the T → G and R → S substitutions found within the STRTR pentapeptide motif (S-57 GRTS-61 in ROCT), as noted by other investigators (56). The T → G-58 replacement in ROCT removes a side chain and, consequently, a potential interaction between CP and the -OH group of this chain. This could weaken CP or inhibitor binding to the enzyme and lead to lower affinity and catalytic efficiency, as reported by Templeton et al. (82). Furthermore, the T-53 residue occurs at the beginning of helix 2 in the *E. coli* ACT (36), and its replacement in ROCT with G-58 (a helix breaker) could prevent helix initiation at this point and locally distort the conformation of the active site. The R → S-62 substitution has precedent in the hamster ACT (46) and removes a basic residue from the vicinity of the CP-binding cleft, and this could negate the possibility of nucleophilic attack postulated to occur during the irreversible inactivation of OCT by octidine (82). The substitution of L-47 (a neutral residue) for basic residues (either arginine or lysine) in all other OCTs (Fig. 5) could be considered in the same vein. However, in the three-dimensional structure of ACT, this position is distant from CP and from the phosphonate group in the enzyme's substrate or inhibitor phosphonacetyl aspartate. The functional significance of the E → F-65 substitution is not obvious. The Q or H → R-85 substitution is very close to S-80 of the *E. coli* ACT, which interacts with CP. Interestingly, the H → N substitution at the corresponding position in the mouse OCT is responsible for the Spf (sparse fur) phenotype and changes the enzyme's pH optimum from 7.7 to 9.5 (89). The occurrence of alanine at position 106 in ROCT has precedent in a site-directed mutant of the *P. aeruginosa* ArcB protein (E-105 → A in our numbering system) which reduces the enzyme's cooperative binding of CP and enables the enzyme to function as both catabolic and anabolic *in vivo* (3). It is unlikely that ROCT functions catabolically *in vivo* since the enzyme's K_m for CP (0.0 mM [82] or 2.8 mM [34]) is uncharacteristic of the high K_m of ArcB for this substrate (38 mM [3]) and *P. syringae* pv. phaseolicola lacks a functional arginine deiminase (75). Other investigators (34) reported that ROCTs from other *P. syringae* pv. phaseolicola strains do not catalyze the reverse reaction *in vitro*.

argK transcription and regulation. We identified three *argK*-specific transcripts and a transcription start point, near the putative ROCT initiation codon, by Northern blot (Fig. 6A) and primer extension analysis (Fig. 6B), respectively. The results of RNA sizing indicated that a small (presumably monocistronic) and two larger (potentially bi- or multicistronic) *argK* mRNAs exist in the cells. We do not know whether the smaller transcripts constitute cleavage products of the larger ones or independently synthesized species. Whereas the promoter region identified in our experiments must certainly be utilized for the synthesis of *argK*-specific mRNA, an additional promoter(s) and initiation point(s) lying further upstream may contribute to *argK* expression. Multiple transcripts have been observed for two other genes in *P. syringae* pv. phaseolicola, namely, the *argF* gene encoding SOCT (27) and the *hrpRS* operon encoding a regulatory protein(s) (17). It is possible that multiple transcription is a common mechanism for regulatory fine tuning

in this bacterium. In the case of *argK*, we examined conditions that are known to regulate the level of ROCT (growth temperature [33, 79, 83]) or other bacterial OCTs (medium composition [8]). Growth at 21°C in MM or at 28°C in KB medium did not change the number or size of the transcripts (data not shown) or the transcription start point detected by the K5 primer (Fig. 6B).

The above results suggested that if *argK* expression is regulated at the transcriptional level, it would be quantitative in nature. The *argK* promoter located upstream of the *argK* frame showed a distinct pattern of regulation. First, increase in temperature from 21 to 28°C caused a 28% decrease in the level of PhoA. This reduction was smaller in magnitude than previously reported for ROCT activity caused by elevated temperature (73% from 22 to 30°C [33]). Although reporter protein activity is not a direct measure of transcription, it is possible that the amplitude of temperature regulation differs between strains. Alternatively, posttranscriptional processes or the activity of the putative promoter(s) driving expression of the larger mRNAs observed may be temperature regulated. Second, contrasting with the fact that the anabolic OCTs of most bacteria (8), including the SOCT of *P. syringae* pv. phaseolicola (82), are repressed by arginine, the *argK* promoter was stimulated in arginine-supplemented cultures. Stimulation occurred at both high and low temperatures but to a different degree (47% at 21°C and over 100% at 28°C). The greater activation at 28°C effectively canceled the apparent repression of the *argK* promoter by elevated temperature in the minimal medium. Templeton et al. (82) concluded that arginine did not repress the level of ROCT activity, and their data show a slight (about 12%) increase by arginine at 18°C. Since the extracts used by these investigators were from a Tox⁺ strain and presumably contained a mixture of ROCT and SOCT, greater stimulation by arginine could not have been observed because of the concurrent repression of the sensitive enzyme in arginine-supplemented medium. Although the apparent induction of the *argK* promoter by arginine seems paradoxical, it has precedents. In *E. coli* B and in *B. subtilis* (during the early stationary phase), addition of arginine results in increased OCT biosynthesis (8).

The possibility that the Northern and primer extension analyses presented above produced spurious results due to the presence of the second OCT gene (*argF*) encoding the phaseolotoxin-sensitive enzyme in strain NPS3121 is considered unlikely for the following reasons. (i) The two genes have only 44% homology in the coding regions (Table 3), where the degree of homology is likely to be highest; (ii) there is no detectable hybridization between the two genes under less stringent conditions used in a previous study (66) compared with the hybridization conditions used here; (iii) the longest uninterrupted regions of perfect matches between the *argK* and *argF* coding regions are limited to single, nonadjacent stretches of 9 and 8 nucleotides each occurring once; (iv) the K5 primer matches the *argF* RNA poorly; in the best matching position, only the 5'-terminal 9 of the 17 bases match the *argK* sequence (27); the K5 primer has a very poor match at the position of the *argF* message which corresponds to the K5-binding site on *argK*.

Functional expression of ROCT in tobacco. The high level of ROCT activity in leaf extracts from transgenic plants expressing *argK* RNA, together with the distinct shift in the pH activity profile of the OCT from transformant 21A, clearly establish that ROCT was expressed in a fully functional form in the plants. This conclusion is further supported by the demonstration of ROCT activity in the prog-

eny from the cross between the II-3.2 transformant and Glurk tobacco, the presence of significantly higher OCT specific activity in the transgenic extracts, and the absence of chlorosis in leaves of transgenic plants treated with toxin. Although chlorosis development in untransformed SR1 plants was not regularly reproducible after toxin application, it is interesting that even group II plants never showed chlorosis. Whereas the efficiency of signal peptide processing and cellular location remain to be investigated, the bacterial enzyme was stable and catalytically active in plants and retained its native resistance to phaseolotoxin. Considering that ROCT is a trimeric enzyme (34), plant OCTs are multimeric (trimeric [76] or tetrameric [1]), and some bacterial OCTs can form functional heterotrimers (8), the lack of coincident maxima in the three pH activity profiles raises the possibility of hybrid plant-bacterium enzyme multimers.

The functional expression of the *argK* gene in higher plants susceptible to *P. syringae* pv. *phaseolicola* is agronomically and scientifically important. Halo blight affects a major legume crop, and the ability to produce phaseolotoxin can be genetically transferred to other *P. syringae* pathovars (27). Additionally, the transgenic tobacco plants offer an opportunity to investigate several pathophysiological aspects of toxin action that are presently not understood: the physiological mechanism of chlorosis development (85); the accumulation of amino acids that are metabolically unrelated to the arginine pathway in toxin-treated plants (68); the inability of a *tox* mutant of the pathogen to move systemically in the plant (64); the suppression of mature tissue resistance (59); the susceptibility of some tolerant cultivars to infection after toxin treatment (23, 59); and the inhibition of shoot and root meristem growth associated with bean halo blight.

ACKNOWLEDGMENTS

The assistance of Yannis Papanikolaou in the OCT alignments and Renate Gressman and Andrei Kajava in the examination of the three-dimensional structure of OCT is acknowledged.

REFERENCES

1. Acaster, M. A., S. Scott-White, and P. D. J. Weitzman. 1989. Carbamoyltransferase reactions in plants. A survey for enzymatic diversity and the potential for herbicidal activity of transition state analogue inhibitors. *J. Exp. Bot.* **219**:1121-1125.
2. An, G. 1986. Development of plant promoter expression vectors and their use for analysis of differential activity of nopaline synthase promoter in transformed tobacco cells. *Plant Physiol.* **81**:86-91.
3. Baur, H., C. Tricot, V. Stalon, and D. Haas. 1990. Converting catabolic ornithine carbamoyltransferase to an anabolic enzyme. *J. Biol. Chem.* **265**:14728-14731.
4. Bradford, M. M. 1976. A rapid and sensitive method for the quantitation of microgram quantities of protein utilizing the principle of protein-dye binding. *Anal. Biochem.* **72**:248-254.
5. Brinkman, E., and J. Beckwith. 1975. Analysis of the regulation of *Escherichia coli* alkaline phosphatase synthesis using deletions and ϕ -80 transducing phages. *Mol. Biol.* **96**:307-316.
6. Church, G. M., and W. Gilbert. 1988. Genomic sequencing. *Proc. Natl. Acad. Sci. USA* **81**:1991-1995.
7. Cundliffe, E. 1989. How antibiotic-producing organisms avoid suicide. *Annu. Rev. Microbiol.* **43**:207-233.
8. Cunin, R., N. Glandsdorff, A. Pierard, and V. Stalon. 1986. Biosynthesis and metabolism of arginine in bacteria. *Microbiol. Rev.* **50**:314-352.
9. Davis, R. W., D. Botstein, and J. R. Roth. 1980. Advanced bacterial genetics. A manual for genetic engineering. Cold Spring Harbor Laboratory, Cold Spring Harbor, N.Y.
10. Deblaere, R., A. Reynaerts, H. Hoftte, J.-P. Hernalsteens, J. Leemans, and M. Van Montague. 1987. Vectors for cloning in plant cells. *Methods Enzymol.* **153**:277-292.
11. Del Sal, G., G. Manioletti, and C. Schneider. 1988. A one tube plasmid DNA mini-preparation suitable for sequencing. *Nucleic Acids Res.* **16**:9878.
12. De Ruiter, H., and C. Kolloffel. 1985. Properties of ornithine carbamoyltransferase from *Pisum sativum* L. *Plant Physiol.* **77**:695-699.
13. De Vos, P., and J. De Ley. 1983. Intra- and intergeneric similarities of *Pseudomonas* and *Xanthomonas* ribosomal ribonucleic acid cistrons. *Int. J. Syst. Bacteriol.* **33**:487-509.
14. Ditta, G. W., S. Stansfield, D. Corbin, and D. R. Helinski. 1984. Broad host range DNA cloning system for gram-negative bacteria: construction of a gene bank of *Rhizobium meliloti*. *Proc. Natl. Acad. Sci. USA* **87**:7347-7351.
15. Durbin, R. D., and P. J. Langston-Unkefer. 1988. The mechanisms of self-protection against bacterial phytochemicals. *Annu. Rev. Phytopathol.* **26**:313-329.
16. Eid, S., Y. Waly, and A. T. Abdelal. 1974. Separation and properties of two ornithine carbamoyltransferases from *Pisum sativum* seedlings. *Phytochemistry* **13**:99-102.
17. Fellay, R., and N. J. Panopoulos. Unpublished data.
18. Ferguson, A. R., and J. S. Johnston. 1980. Phaseolotoxin: chlorosis, ornithine accumulation and inhibition of ornithine carbamoyltransferase from different plants. *Physiol. Plant Pathol.* **16**:269-275.
19. Ferguson, A. R., J. S. Johnston, and R. E. Mitchell. 1980. Resistance of *Pseudomonas syringae* pv. *phaseolicola* to its own toxin, phaseolotoxin. *FEMS Lett.* **7**:123-125.
20. Gavel, Y., and G. von Heijne. 1990. A conserved cleavage site motif in chloroplast transit peptides. *FEBS Lett.* **261**:455-458.
21. Gilman, M. 1987. Preparation of bacterial RNA, p. 4.4.1-4.4.4. *In* F. M. Ausubel, R. Brent, R. E. Kingston, D. D. Moore, J. G. Seidman, J. A. Smith, and K. Struhl (ed.), *Current protocols in molecular biology*, vol. I. John Wiley & Sons, Inc., New York.
22. Glen, E., and A. Maretzki. 1977. Properties and subcellular distribution of two partially purified ornithine carbamoyltransferases in cell suspensions of sugar cane. *Plant Physiol.* **60**:122-126.
23. Gnanamanickam, S. S., and S. S. Patil. 1977. Phaseolotoxin suppresses bacterially induced hypersensitive reaction and phytoalexin synthesis in bean cultivars. *Physiol. Plant Pathol.* **10**:169-179.
24. Gouaux, J. E., and W. N. Lipscomb. 1988. Three-dimensional structure of carbamoylphosphate and succinate bound to aspartate carbamoyltransferase. *Proc. Natl. Acad. Sci. USA* **85**:4205-4208.
25. Grimm, C. G., R. D. Frederick, D. Dahlbeck, N. J. Panopoulos, and B. J. Staskawicz. Unpublished data.
26. Guerineau, F., S. Woolston, L. Brooks, and P. Mullineaux. 1988. An expression cassette for targeting foreign proteins into chloroplasts. *Nucleic Acids Res.* **16**:11380.
27. Hatziloukas, E., and N. J. Panopoulos. Unpublished data.
28. Higgins, D. G., and P. M. Sharp. 1989. CLUSTAL: a package performing multiple sequence alignments on a microcomputer. *Gene* **73**:237-244.
29. Horwich, A. L., W. A. Fenton, K. R. Williams, F. Kalousek, J. P. Kraus, R. F. Doolittle, W. Konigsberg, and L. E. Resenber. 1984. Structure and expression of a complementary DNA for the nuclear coded precursor of human mitochondrial ornithine transcarbamylase. *Science* **224**:1068-1074.
30. Houghton, J. E., D. E. Bencini, G. A. O'Donovan, and J. R. Wild. 1984. Protein differentiation: a comparison of aspartate transcarbamoylase and ornithine transcarbamoylase from *Escherichia coli* K-12. *Proc. Natl. Acad. Sci. USA* **81**:4864-4868.
31. Huygen, R., M. Crabeel, and N. Glandsdorff. 1987. Nucleotide sequence of the ARG3 gene of the yeast *Saccharomyces cerevisiae* encoding ornithine carbamoyltransferase. Comparison with other carbamoyltransferases. *Eur. J. Biochem.* **166**:371-377.
32. Itoh, Y., L. Soldati, V. Stalon, P. Flamagne, Y. Terawaki, T. Leisinger, and D. Haas. 1988. Anabolic ornithine carbamoyltransferase of *Pseudomonas aeruginosa*: nucleotide sequence

- and transcriptional control of the *argF* structural gene. *J. Bacteriol.* **170**:3225–3234. (Erratum, **172**:2199.)
33. Jahn, J., J. Sauerstein, and G. Reuter. 1985. Detection of two ornithine carbamoyltransferases in a phaseolotoxin-producing strain of *Pseudomonas syringae* pv. *phaseolicola*. *J. Basic Microbiol.* **25**:543–546.
 34. Jahn, J., J. Sauerstein, and G. Reuter. 1987. Characterization of two ornithine carbamoyltransferases from *Pseudomonas syringae* pv. *phaseolicola*, the producer of phaseolotoxin. *Arch. Microbiol.* **147**:174–178.
 35. Kantrowitz, E. R., and W. N. Lipscomb. 1988. *Escherichia coli* aspartate transcarbamylase: the relation between structure and function. *Science* **241**:669–674.
 36. Ke, H.-M., R. B. Honzatko, and W. N. Lipscomb. 1984. Structure of unliganded aspartate carbamoyltransferase of *Escherichia coli* at 2.6 Å resolution. *Proc. Natl. Acad. Sci. USA* **81**:4037–4040.
 37. King, E. O., M. K. Wood, and D. E. Raney. 1954. Two simple media for the demonstration of pyocyanin and fluorescein. *J. Lab. Clin. Med.* **44**:301–307.
 38. Kingston, R. E. 1987. Primer extension, p. 4.8.1–4.8.3. In F. M. Ausubel, R. Brent, R. E. Kingston, D. D. Moore, J. G. Seidman, J. A. Smith, and K. Struhl (ed.), *Current protocols in molecular biology*, vol. 1. John Wiley & Sons, Inc., New York.
 39. Kinney, D. M., and C. J. Lusty. 1989. Arginine restriction induced by δ -*N*-(phosphonacetyl)-L-ornithine signals increased expression of *HIS3*, *TRP5*, *CPA1*, and *CPA2* in *Saccharomyces cerevisiae*. *Mol. Cell. Biol.* **9**:4882–4888.
 40. Krause, K. L., K. W. Volz, and W. N. Lipscomb. 1985. Structure at 2.9 Å resolution of aspartate carbamoyltransferase complexed with the bisubstrate analogue *N*-(phosphonacetyl)-L-aspartate. *Proc. Natl. Acad. Sci. USA* **82**:1643–1647.
 41. Kuo, L. C., C. Caron, S. Lee, and W. Hertzberg. 1990. Zn⁺⁺ regulation of ornithine transcarbamoylase. II. Metal binding site. *J. Mol. Biol.* **211**:271–280.
 42. Kuo, L. C., W. Hertzberg, and W. N. Lipscomb. 1985. Substrate specificity and protonation state of ornithine carbamoyltransferase as determined by pH studies. *Biochemistry* **24**:4754–4761.
 43. Kuo, L. C., A. W. Miller, S. Lee, and C. Kozuma. 1988. Site directed mutagenesis of *Escherichia coli* ornithine transcarbamylase: role of arginine 57 in substrate binding and catalysis. *Biochemistry* **27**:8823–8832.
 44. Kuo, L. C., and B. A. Seaton. 1989. X-ray diffraction analysis on single crystals of recombinant *Escherichia coli* ornithine transcarbamylase. *J. Biol. Chem.* **264**:16246–16248.
 45. Laemmli, U. K. 1970. Cleavage of structural proteins during the assembly of the head of bacteriophage T4. *Nature (London)* **227**:680–685.
 46. Major, J. G., Jr., M. E. Wales, J. E. Houghton, J. A. Maley, J. N. Davidson, and J. R. Wild. 1989. Molecular evolution of enzyme structure: construction of a hybrid hamster/*Escherichia coli* aspartate transcarbamoylase. *J. Mol. Evol.* **28**:442–450.
 47. Maniatis, T., E. F. Fritsch, and J. Sambrook. 1982. *Molecular cloning: a laboratory manual*. Cold Spring Harbor Laboratory, Cold Spring Harbor, N.Y.
 48. Martin, P. R., J. W. Cooperider, and M. H. Mulks. 1990. Sequence of the *argF* gene encoding ornithine transcarbamoylase from *Neisseria gonorrhoeae*. *Gene* **94**:139–140.
 49. Melchers, L. S., T. J. G. Regensburg-Tuint, B. B. Bourret, N. J. A. Sedee, R. A. Schilperroort, and T. J. Hooykass. 1989. Membrane topology and functional analysis of the sensory protein VirA of *Agrobacterium tumefaciens*. *EMBO J.* **8**:1919–1925.
 50. Messing, J. 1983. New M13 vectors for cloning. *Methods Enzymol.* **101**:10–89.
 51. Miller, J. H. 1972. *Experiments in molecular genetics*. Cold Spring Harbor Laboratory, Cold Spring Harbor, N.Y.
 52. Mindrinos, M. N., L. G. Rahme, R. T. Frederick, E. Hatziloukas, C. Grimm, and N. J. Panopoulos. 1990. Structure, function, regulation, and evolution of genes involved in the expression of pathogenicity, the hypersensitive response, and phaseolotoxin immunity in the bean halo blight pathogen, p. 74–81. In A. M. Chakrabarty, B. Iglewski, S. Kaplan, and S. Silver (ed.), *Pseudomonas: biotransformations, pathogenesis, and evolving biotechnology*. American Society for Microbiology, Washington, D.C.
 53. Mitchell, R. E. 1984. The relevance of non-host-specific toxins in the expression of virulence by pathogens. *Annu. Rev. Phytopathol.* **22**:215–245.
 54. Mitchell, R. E., and R. L. Bielecki. 1977. Involvement of phaseolotoxin in haloblight of beans. Transport and conversion to functional toxin. *Physiol. Plant Pathol.* **19**:227–235.
 55. Moore, R. E., W. P. Niemczura, O. C. H. Kwok, and S. S. Patil. 1984. Inhibitors of ornithine carbamoyltransferase from *Pseudomonas syringae* pv. *phaseolicola*. Revised structure of phaseolotoxin. *Tetrahedron Lett.* **25**:3931–3934.
 56. Mosqueda, G., G. van den Broek, O. Saucedo, A.-M. Bailey, A. Alvarez-Morales, and L. Herrera-Estrella. 1990. Isolation and characterization of a gene from *Pseudomonas syringae* pv. *phaseolicola* encoding a phaseolotoxin-insensitive ornithine carbamoyltransferase. *Mol. Gen. Genet.* **222**:461–466.
 57. Mountain, A., M. C. M. Smith, and S. Baumberg. 1990. Nucleotide sequence of the *Bacillus subtilis argF* gene encoding ornithine carbamoyltransferase. *Nucleic Acids Res.* **18**:4594.
 58. Muto, A., and S. Osawa. 1987. The guanine and cytosine content of genomic DNA and bacterial evolution. *Proc. Natl. Acad. Sci. USA* **84**:166–169.
 59. Oguchi, T., B. V. Gantotti, G. K. H. Ho, and S. Patil. 1981. *Phaseolus vulgaris*-*Pseudomonas syringae* pv. *phaseolicola* system: role of host tissue age and pathogenic toxin in establishment of pathogen in host, p. 288–294. In C. Lozano (ed.), *Proceedings of the Vth International Conference on Plant Pathogenic Bacteria*. Centro Internacional de Agricultura Tropical, Cali, Colombia.
 60. Panopoulos, N. J., E. Hatziloukas, D. A. Baertlein, S. E. Lindow, T. H. Chen, and M. N. Mindrinos. 1991. *Pseudomonas syringae*-plant interactions: mechanisms and genes for crop protection. In G. Tzotzos (ed.), *Biotechnology in the 1990's*, in press. International Center for Genetic Engineering and Biotechnology, Trieste, Italy.
 61. Panopoulos, N. J., and R. C. Peet. 1985. The molecular genetics and plasmids of plant pathogenic bacteria. *Annu. Rev. Phytopathol.* **23**:381–419.
 62. Panopoulos, N. J., and B. J. Staskawicz. 1981. Genetics of production, p. 74–107. In R. D. Durbin (ed.), *Toxins and plant disease*. Academic Press, Inc., New York.
 63. Pastra-Landis, S. C., J. Foote, and E. R. Kantrowitz. 1981. An improved colorimetric assay for aspartate and ornithine transcarbamoylases. *Anal. Biochem.* **118**:358–363.
 64. Patil, S. S., A. C. Hayward, and R. Emmons. 1974. An ultraviolet induced nontoxic mutant of *Pseudomonas phaseolicola* of altered pathogenicity. *Phytopathology* **64**:590–595.
 65. Peet, R. C., P. B. Lindgren, D. K. Willis, and N. J. Panopoulos. 1986. Genetic analysis of phaseolotoxin production by *P. syringae* pv. *phaseolicola*. *J. Bacteriol.* **166**:1096–1105.
 66. Peet, R. C., and N. J. Panopoulos. 1987. Ornithine carbamoyltransferase genes and phaseolotoxin immunity in *Pseudomonas syringae* pv. *phaseolicola*. *EMBO J.* **6**:3585–3591.
 67. Peet, R. C., and N. J. Panopoulos. Unpublished data.
 68. Rudolph, K., and M. A. Stahmann. 1966. The accumulation of L-ornithine in haloblight infected bean plants (*Phaseolus vulgaris*), induced by the toxin of the pathogen, *Pseudomonas phaseolicola* (Burkh.) Dowson. *Phytopathol. Z.* **57**:29–46.
 69. Sanger, F., and A. R. Coulson. 1978. The use of thin acrylamide gels for DNA sequencing. *FEBS Lett.* **87**:107–110.
 70. Sanger, F., S. Nicklen, and A. R. Coulson. 1977. DNA sequencing with chain-terminating inhibitors. *Proc. Natl. Acad. Sci. USA* **74**:5463–5467.
 71. Savioz, A., D. J. Jeenes, H. P. Koscher, and D. Haas. 1990. Comparison of *proC* and other housekeeping genes of *Pseudomonas aeruginosa* and *Escherichia coli*. *Gene* **86**:107–111.
 72. Schachman, H. K., C. D. Pauza, M. Navre, M. J. Karels, L. Wu, and Y. R. Yang. 1984. Location of amino acid alterations in mutants of aspartate transcarbamoylase: structural aspects of interallelic complementation. *Proc. Natl. Acad. Sci. USA* **81**:

- 115–119.
73. Scherer, S. E., G. Veres, and C. T. Caskey. 1988. The genetic structure of mouse ornithine transcarbamylase. *Nucleic Acids Res.* **16**:1593–1601.
 74. Schneider, K., and C. F. Beck. 1987. New expression vectors for identifying and testing signal structures for initiation and termination of transcription. *Methods Enzymol.* **153**:452–461.
 75. Schroth, M. N., D. C. Hildebrand, and N. J. Panopoulos. 1992. Phytopathogenic and related plant-associated pseudomonads, p. 3104–3131. In A. Balows, H. G. Truper, M. Dworkin, W. Harder, and K. H. Schleifer (ed.), *The prokaryotes*. Springer-Verlag, New York.
 76. Slocum, R. D., and D. P. Richardson. 1991. Purification and characterization of ornithine transcarbamylase from pea (*Pisum sativum*). *Plant Physiol.* **96**:262–268.
 77. Staskawicz, B. J., and N. J. Panopoulos. 1979. A rapid and sensitive microbiological assay for phaseolotoxin. *Phytopathology* **69**:663–666.
 78. Staskawicz, B. J., and N. J. Panopoulos. 1980. Phaseolotoxin transport in *Escherichia coli* and *Salmonella typhimurium* via the oligopeptide permease. *J. Bacteriol.* **142**:474–479.
 79. Staskawicz, B. J., N. J. Panopoulos, and N. J. Hoogenraad. 1980. Phaseolotoxin-insensitive ornithine carbamoyltransferase of *Pseudomonas syringae* pv. *phaseolicola*: basis for immunity to phaseolotoxin. *J. Bacteriol.* **142**:720–723.
 80. Stebbins, J. W., W. Xu, and E. Kantrowicz. 1989. The residues involved in binding and catalysis in the carbamyl phosphate binding site of *Escherichia coli* aspartate transcarbamylase. *Biochemistry* **28**:2592–2600.
 81. Takiguchi, M., S. Miura, M. Mori, M. Tatibana, S. Nagata, and Y. Kaziro. 1984. Molecular cloning and nucleotide sequence of cDNA for rat ornithine carbamoyltransferase precursor. *Proc. Natl. Acad. Sci. USA* **81**:7412–7416.
 82. Templeton, M. D., R. E. Mitchell, P. A. Sullivan, and G. Shepherd. 1985. The inactivation of ornithine transcarbamoylase by *N*⁶(*N*'-sulpho-diaminophosphinyl)-L-ornithine. *Biochem. J.* **228**:347–352.
 83. Templeton, M. D., P. A. Sullivan, and G. Shepherd. 1985. Phaseolotoxin-insensitive L-ornithine transcarbamoylase from *Pseudomonas syringae* pv. *phaseolicola*. *Physiol. Mol. Plant Pathol.* **29**:393–403.
 84. Tricot, C., J.-L. de Coen, P. Momin, P. Falmagne, and V. Stalon. 1988. Evolutionary relationships among bacterial carbamoyltransferases. *J. Gen. Microbiol.* **135**:2453–2464.
 85. Turner, J. G., and R. E. Mitchell. 1985. Association between symptom development and inhibition of ornithine carbamoyltransferase in bean leaves treated with phaseolotoxin. *Plant Physiol.* **79**:468–473.
 86. Upshall, A., T. Gilbert, G. Saari, P. J. O'Hara, P. Weglenski, B. Berse, K. Miller, and W. E. Timberlake. 1986. Molecular analysis of the *argB* gene of *Aspergillus nidulans*. *Mol. Gen. Genet.* **204**:349–354.
 87. Van Vliet, F., A. Boyen, and N. Glandsdorff. 1988. On interspecies gene transfer: the case of the *argF* gene of *Escherichia coli*. *Ann. Inst. Pasteur Microbiol.* **139**:493–496.
 88. Van Vliet, F., F. R. Cunin, A. Jacobs, J. Piette, M. Lauwereys, A. Pierard, and N. Glandsdorff. 1984. Evolutionary divergence of genes for ornithine carbamoyltransferase—complete sequence and mode of regulation of the *E. coli argF* gene; comparison of *argI* with *argF* and *pyrB*. *Nucleic Acids Res.* **12**:6277–6289.
 89. Veres, G., R. A. Gibbs, S. E. Sherer, and C. T. Caskey. 1987. The molecular basis of the sparse fur mouse mutation. *Science* **237**:415–417.
 90. Verword, T. C., M. M. Dekker, and A. Hokema. 1989. A small scale procedure for the rapid isolation of plant RNAs. *Nucleic Acids Res.* **17**:2362.
 91. Voltz, K. W., K. L. Krause, and W. N. Lipscomb. 1986. The binding of *N*-(phosphonacetyl)-L-aspartate to aspartate transcarbamoylase of *Escherichia coli*. *Biochem. Biophys. Res. Commun.* **136**:822–826.
 92. Wild, J. R., and M. E. Whales. 1990. Molecular evolution and genetic engineering of protein domains involving aspartate transcarbamoylase. *Annu. Rev. Microbiol.* **44**:193–218.
 93. Xu, W., and E. R. Kantrowitz. 1989. Function of threonine-55 in the carbamoyl phosphate binding site of *Escherichia coli* aspartate transcarbamoylase. *Biochemistry* **28**:9937–9943.